

UNDERSTANDING THE BIOLOGICAL BASIS OF COGNITIVE AGING:

THE ROLE OF INHIBITORY INTERNEURONS

By

JESSICA CHERI BURKHART

A Thesis Submitted to the Honors College

In Partial Fulfillment of the Bachelors degree
With Honors in

Neuroscience and Cognitive Science

THE UNIVERSITY OF ARIZONA

MAY 2015

Approved by



Dr. Carol Barnes

Department of Psychology

Abstract

Previous studies reveal decreases in hippocampal interneuron cell densities during normal aging. However, considerable variation in results exists within the literature. Overall, interneuron populations show either decreases or conservation in cell numbers expressing calcium binding proteins parvalbumin (PV) and calbindin (CB), and neuropeptides somatostatin (SOM) and neuropeptide Y (NPY) in hippocampal subregions of CA1, CA3, dentate granule cell layer, and dentate hilus. Notably, only few of the past aging studies showed correlations in cell loss with behavioral impairments in aged animals. This issue was addressed in the present study using male, young and old Fischer 344 rats, that were behaviorally characterized on four tasks before immunohistochemical staining and cell type quantification. Rats performed the Morris Watermaze, W-Track Continuous Spatial Alternation Task, Spontaneous Object Recognition (SOR) task, and Temporal Object Recognition (TOR) task. The old rats showed age-related deficits only in hippocampal-dependent memory tasks. Immunofluorescent imaging revealed an increase in SOM-immunoreactive interneurons in the dentate granule cell layer, as well as an increase in NPY expression in the dentate hilus. All other regions in which neurons were quantified showed no changes in any of the selected interneuron types examined. Contrary to previous findings, we found no decreases in interneuron populations anywhere in the hippocampus.

Thesis Roles & Responsibilities

CONTRIBUTORS:

- ❖ Jessica Burkhart: Undergraduate Honors Student
- ❖ Chelsea Takamatsu: Undergraduate Honors Student
- ❖ Daniel Gray: Graduate Research Assistant
- ❖ Dr. Carol A. Barnes: Honors Mentor & Principle Investigator

June 2014:

- 24 rats were received from the National Institute of Aging.

June 2014 - July 2014:

- Chelsea Takamatsu, the Barnes lab technicians, and the summer research associates behaviorally trained the rats in four behavior tasks: the Morris Watermaze, the W-Track Spontaneous Alternation Task, Spontaneous Object Recognition (SOR) task, and Temporal Object Recognition (TOR) task.

August 2014:

- Chelsea Takamatsu and graduate student, Daniel Gray, sacrificed 13 rats.

August - September 2014:

- Chelsea Takamatsu sliced 3500 brain sections from the sacrificed rats' hippocampi and the prefrontal cortices on the microtome.

October - November 2014:

- Chelsea Takamatsu and Jessica Burkhart separated out every ninth tissue per animal of the hippocampus and prefrontal cortex, respectively, and mounted them onto slides for Nissl staining.

December 2014:

- Chelsea Takamatsu, Jessica Burkhart, and Daniel Gray Nissl stained the slides of hippocampus and prefrontal cortex tissues.
- Chelsea Takamatsu and Jessica Burkhart completed over 30 hours of SOR and TOR scoring in order to analyze the behavior data.

January 2015:

- Daniel Gray analyzed the behavior data in order for Chelsea Takamatsu to present the project at the Undergraduate Biology Research Program Annual Poster Session. The behavior results directed the study to solely focus on the hippocampus, moving Jessica Burkhart from the prefrontal cortex portion of the study to join Chelsea Takamatsu in the hippocampus study.
- Chelsea Takamatsu and Jessica Burkhart divided 27 publications and read through the papers, organizing them into a chart that summarized the interneuron literature.

- Chelsea Takamatsu located the coordinates of the Nissl-stained hippocampus tissues relative to Bregma, using the projection microscope and the Paxinos & Watson Brain Atlas.
- Chelsea Takamatsu, Jessica Burkhart, and Daniel Gray used the tissue location coordinates to finalize from where the tissues for immunohistochemistry would be sampled.

February 2015:

- Chelsea Takamatsu and Jessica Burkhart mounted the appropriate tissues for each immunofluorescent stain onto slides.

March 2015:

- Chelsea Takamatsu, Jessica Burkhart, and Daniel Gray performed the immunohistochemistry of the slides stained for parvalbumin, calbindin, somatostatin, and neuropeptide Y.
- Chelsea Takamatsu and Jessica Burkhart coverslipped the slides in preparation for the immunofluorescent imaging.

March - April 2015:

- Chelsea Takamatsu and Jessica Burkhart imaged 96 tissues on the Deconvolution Microscope, which totaled over 100 hours of work.

April 2015:

- Daniel Gray cell counted 3600 fluorescent images, requiring a total of 48 hours of work.
- Chelsea Takamatsu and Jessica Burkhart organized the data into tables for analysis.
- Daniel Gray analyzed the cell count data.
- Jessica Burkhart presented the project at the Neuroscience major poster session.

April-May 2015:

- Chelsea Takamatsu and Jessica Burkhart collaborated in writing their joint thesis, on which Daniel Gray and Dr. Carol Barnes provided feedback.

Understanding the Biological Basis of Cognitive Aging: The Role of Inhibitory Interneurons

J.C. Burkhardt^{1,2}, C. L. Takamatsu^{1,2}, D. T. Gray^{1,2}, C. A. Barnes^{1,2,3}

¹Evelyn F. McKnight Brain Institute; ²ARL Division of Neural Systems, Memory, & Aging;

³Departments of Psychology, Neurology and Neuroscience, University of Arizona, Tucson, AZ

Abstract

Previous studies reveal decreases in hippocampal interneuron cell densities during normal aging. However, considerable variation in results exists within the literature. Overall, interneuron populations show either decreases or conservation in cell numbers expressing calcium binding proteins parvalbumin (PV) and calbindin (CB), and neuropeptides somatostatin (SOM) and neuropeptide Y (NPY) in hippocampal subregions of CA1, CA3, dentate granule cell layer, and dentate hilus. Notably, only few of the past aging studies showed correlations in cell loss with behavioral impairments in aged animals. This issue was addressed in the present study using male, young and old Fischer 344 rats, that were behaviorally characterized on four tasks before immunohistochemical staining and cell type quantification. Rats performed the Morris Watermaze, W-Track Continuous Spatial Alternation Task, Spontaneous Object Recognition (SOR) task, and Temporal Object Recognition (TOR) task. The old rats showed age-related deficits only in hippocampal-dependent memory tasks. Immunofluorescent imaging revealed an increase in SOM-immunoreactive interneurons in the dentate granule cell layer, as well as an increase in NPY expression in the dentate hilus. All other regions in which neurons were quantified showed no changes in any of the selected interneuron types examined. Contrary to previous findings, we found no decreases in interneuron populations anywhere in the hippocampus.

Introduction

As the human lifespan increases and the aged population grows, there is greater concern with memory preservation throughout the lifetime. The hippocampus is a critical structure in the formation of new memories (episodic memory) and memory association processes. Consequently, understanding the biological changes that occur across a lifetime within the hippocampus is necessary before therapies for memory conservation can be developed effectively.

Modulation of neural activity, through maintaining a proper balance between excitatory and inhibitory signals, is essential, as disrupted network firing may result in impaired memory (Wilson et al., 2005a; Yassa et al., 2011). With age, the hippocampus exhibits functional changes in animal subjects and humans, shown by fMRI studies that reveal increased activity in the dentate gyrus / CA3 subregions of the hippocampus (Yassa et al., 2010, 2011). CA3 plays a crucial role in maintaining a computational balance between hippocampal pattern separation and pattern

completion operations. Therefore, CA3 hyperactivity in aged animals may bias the system towards inappropriate pattern completion, so that when older animals are in new environments, they are unable to distinguish their new surroundings from familiar ones, as they inappropriately reuse a previously encoded spatial map rather than creating a new one (Wilson et al., 2005).

A proposed explanation for both aged rodents and primates showing increased baseline firing rates of CA3 principal neurons is reduced inhibitory control of neurons from a loss of GABAergic interneurons (Wilson et al., 2005; Thome et al., 2015). Regulating neural firing of excitatory glutamatergic neurons, these inhibitory interneurons release the neurotransmitter GABA, and are differentiated by their morphological, physiological, and chemical properties. Possessing remarkable diversity, interneuron subclasses express various neurochemical markers, which can be immunohistochemically tagged in order to detect the presence of particular interneuron classes.

Numerous studies in aged rats demonstrate selective losses in the number of specific, chemically-defined GABAergic interneurons throughout the hippocampus. Previous publications on the hippocampal subregions report changes in interneuron population densities that contribute to age-related learning and memory deficits. A literature review of 27 papers guided the current study in determining which types of GABAergic cells to target for our aging study (Supplementary document). We chose to focus on the cells immunoreactive for calcium binding proteins Parvalbumin (PV) and Calbindin (CB) and neuropeptides Somatostatin (SOM) and Neuropeptide-Y (NPY), because these are some of the most predominant interneurons in the hippocampus, and have shown losses in numerous studies. The current literature, however, contains contradictory findings, which is illustrated in table 1). With respect to age-related PV interneuron changes, we would expect to obtain results that follow the general conclusion trends of previous works (Table 1 and supplementary document), namely population conservation or decreases in PV, CB, SOM, and NPY-expressing interneurons in CA1, CA3, the granule cell layer of the dentate gyrus (DG), and the DG hilus (Spiegel et al., 2013; Hattiangady et al., 2005; Shetty and Turner, 1998).

The goal of the current study is to relate interneuron losses in the hippocampus of young and aged rats with age-related behavioral performances in tasks dependent on the medial temporal lobe. A cohort of Fisher 344 rats, six aged (24 months) and six young (9 months), completed four behavior tasks, including the Morris Watermaze, W-Track Spatial Alternation Task, Spontaneous Object Recognition Task, and Temporal Order Recognition Task, to assess animal memory statuses prior to the quantification of cellular changes. Following immunohistochemical preparation and fluorescent microscopy, our rats revealed no decreases in any of the targeted chemical markers in the hippocampus subregions, along with notable increases in density of SOM expressing interneurons in the DG granule cells and NPY expressing interneurons in the DG hilus.

	CA1	CA3	DG	Hilus
SOM	(6) decrease, (17) decrease, (24) decrease, (26) decrease	(6) no change (24) decrease	(24) decrease	(24) decrease
NPY	(7) decrease (11) decrease (24) no change	(7) decrease (11) decrease (24) no change	(7) decrease (11) decrease (24) no change	(2) decrease
CB	(4) decrease (17) decrease (21) decrease	(4) no change (21) decrease	(4) no change	(4) no change (21) decrease
PV	(6) no change (11) no change (12) decrease (16) no change (17) no change (21) decrease (26) no change	(6) no change (11) decrease (16) no change (21) decrease	(6) no change (11) decrease (12) decrease	(21) decrease

2	Cadacio et al. (2003)
4	Dutar et al. (1991)
6	Gavilán et al. (2007)
7	Hattiangady et al. (2005)
11	Kuruba et al. (2011)
12	Lolova and Davidoff (1992)
16	Potier et al. (1994)
17	Potier et al. (2006)
21	Shetty and Turner (1998)
24	Spiegel et al. (2013)
26	Stanley et al. (2012)

Table 1: Selected publications that form the background to the current study. The interneuron subclasses are listed in the left most column of the larger, uppermost table. The hippocampal subregions are listed in the top row. The numbers in the larger table correspond to studies denoted in the lower, smaller table.

Methods

Animal Subjects

Young (9 months, n=6) and aged (24 months, n=6) male Fischer 344 rats were obtained from the colony supported by the National Institute on Aging and were housed in a 12 hour light/dark cycle, climate-controlled colony room. Animals were given regular health inspections and determined healthy during testing. During the W-Maze task the rats were food restricted and maintained at 80% of

their initial weight. At the time of sacrifice, the young and old animals were 11 months and 26 months, respectively.

Behavioral Assessment

Morris Watermaze

This spatial task relies on an intact, functional hippocampus in order to be performed properly. The protocol is divided into a spatial task on days 1 through 4, a probe trial at the end of day 4, and a cue discrimination task on days 5 and 6.

Each animal was placed in a tank of water made opaque with chalk, and was released from one of eight randomly selected entry locations for a maximum of a 60 second trial swim (Figure 1). If the rat found the target platform submerged in one quadrant of the tank using environmental stimuli prior to the 60 second time limit, it was immediately dropped into the tank for a second 60 second trial from another randomly selected entry location. If the time limit was exceeded, the rat sat on the target platform for 30 seconds, in order to observe visual cues in its surroundings, prior to its second 60 second swim. As with the first trial, the second trial was followed by a 30 second waiting period on the platform if the time limit was not met. The two trials were repeated three times per day during the four day spatial task.

The probe trial concluded day 4 testing with a 60 second swim and the platform removed in order to measure the rat's times in each quadrant and proximity to the previous submerged target location during the Spatial Task.

The Cue Discrimination Task on the final two days of Watermaze experimentation were formatted similarly to the Spatial Task, but the platform was visible to the rat after some of the tank water was drained to lower the surface level, and the platform location was randomized on each trial. Three sets of two 60 second trials were completed per day with 30 second rests on the platform following trials when the 60 second time limit was not met. The entry point was randomized on each trial.

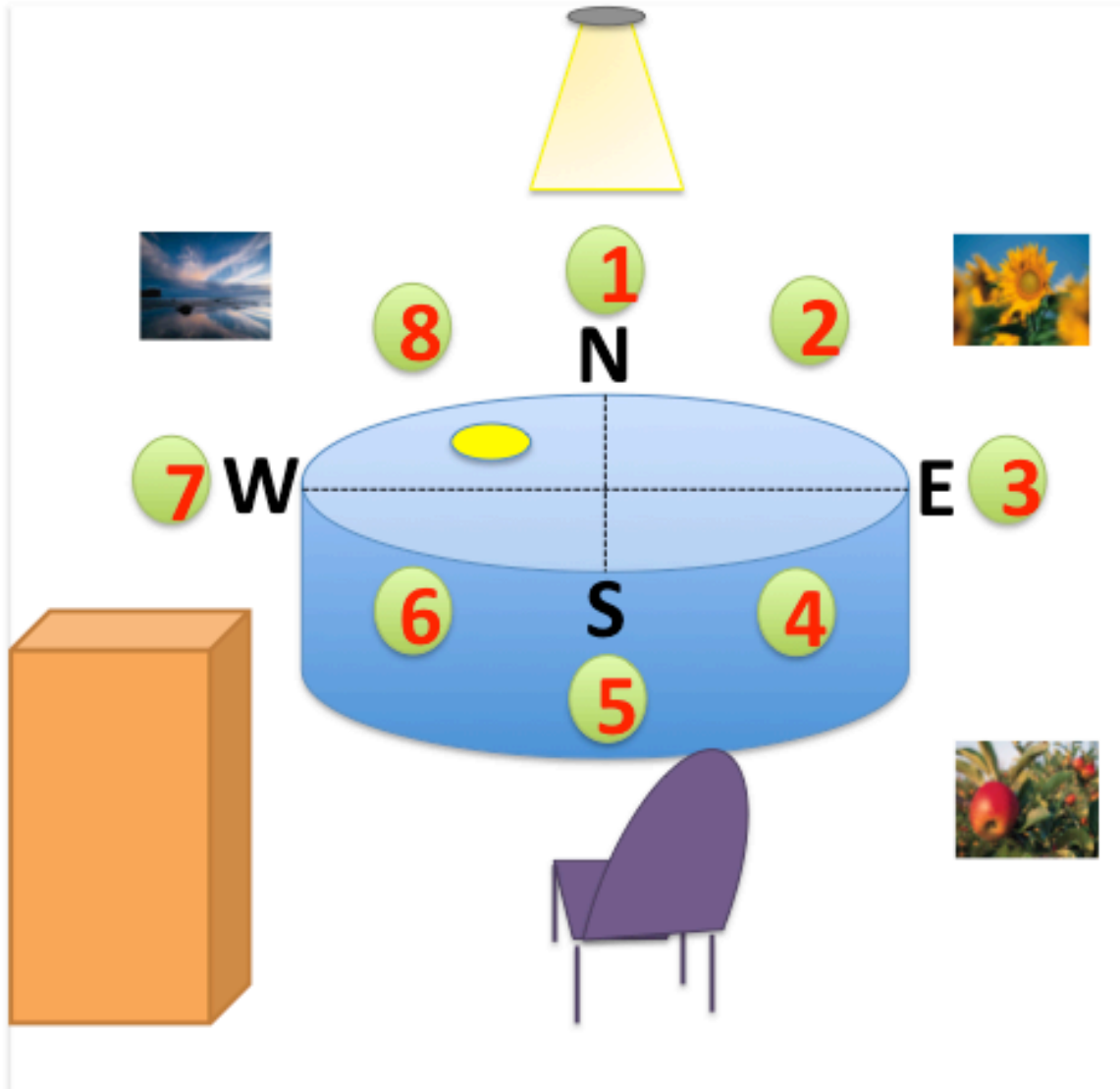


Figure 1: The Hippocampus-dependent Morris Watermaze. A depiction of the Watermaze room with the designated entry locations, cardinal directions, tank quadrants, and environmental stimuli is shown above.

W-Track Continuous Spatial Alternation Task

This behavioral task depends on medial prefrontal cortex – hippocampal neural circuits. Specifically, outbound errors committed during the task reflect impaired spatial working memory reliant on the prefrontal cortex, and inbound errors reflect impaired spatial reference memory reliant on the hippocampus.

Before the W-Track experiment began, the rats were food-deprived and conditioned to run laps on a linear track for a food reward. Once the rat completed at least 40 laps in 15 minutes, it finished linear track pre-training and started testing on the W-Track, during which it ran patterns for 15 minutes daily for 14 consecutive days. The rats were initially placed on the center arm and ran down it for a food reward, after which they selected to run down one of the two outside arms for another rewarded lap (Figure 2). From the outer arm, the rats were rewarded for

returning to center arm, beginning the formation of the “W” pattern. However, the rats were not rewarded for committing inbound errors when they bypassed the center arm and ran from one outside arm to the other. Once the rat returned to the center arm, it was rewarded for running from center arm to the outer arm not initially chosen, correctly moving in the “W” pattern. Alternatively, an outbound error was committed if the rat returned to the outer arm it initially chose and was therefore not rewarded for its mistake.

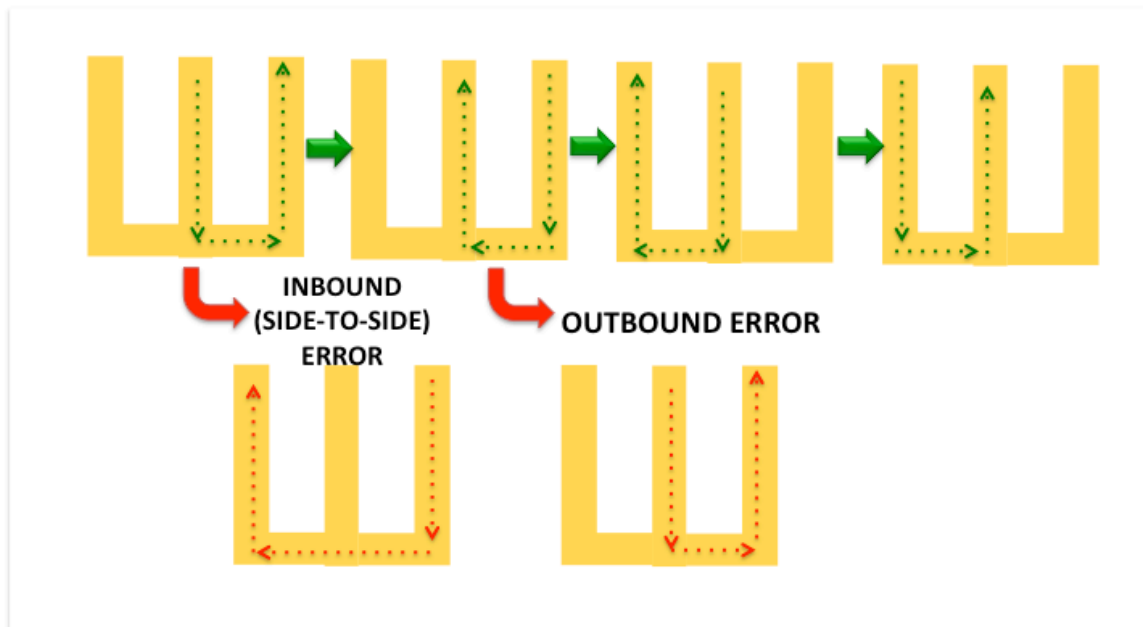


Figure 2: The prefrontal cortex and hippocampus-dependent W-Track Continuous Spatial Alternation Task. Green arrows show correct running patterns that were rewarded. Red arrows show incorrect running errors that were not rewarded. Outbound errors signified impaired spatial working memory in the prefrontal cortex. Inbound errors represented impaired spatial reference memory in the hippocampus.

Spontaneous Object Recognition Task

This task is perirhinal cortex-dependent and broken up into two phases: habituation and recognition, with the recognition phase further divided into object familiarization and test phases. Habituation took place on days 1 and 2, when each rat underwent 10 minutes of exposure to an empty box to become acquainted with it. Days 3 through 5 comprised the recognition phase (Figure 3), which started with a four-minute object familiarization, during which the rats were placed in the same box to which they were previously habituated, along with two identical objects. Next, the rats were removed from the box for a two minute, 15 minute, and 2 hour delay on days 3, 4, and 5, respectively. Following the delay, the rats were placed in the box for the four-minute test phase with a third replica of the object presented during object familiarization, along with a novel object.

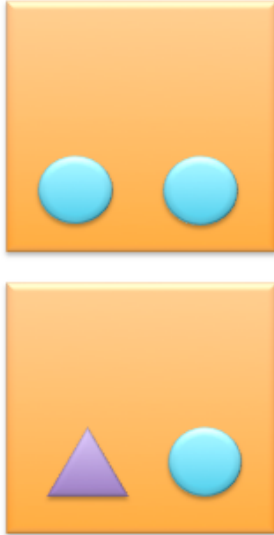


Figure 3: The Perirhinal Cortex-dependent Spontaneous Object Recognition Task. The top and bottom boxes show the apparatus in the Object Familiarization Phase and Test Phase, respectively, of the Recognition part of the protocol. There was a variable delay of 2 minutes, 15 minutes, or 2 hours, following the Object Familiarization Phase.

Temporal Order Recognition Task

This behavioral task requires a functional prefrontal cortex. Similar to the Spontaneous Object Recognition Task, the task was completed in a box, and thus had a habituation phase on days 1 and 2 for 10 minutes in the empty box. The testing phase was completed on Day 3 (Figure 4), beginning with sample phase 1, when the rat was placed in the same familiarized box for four minutes with two identical objects. The rat was taken out of the box for a one hour delay before completing sample phase 2 for four minutes in the box with two identical, but different objects from those presented in the first sample phase. A three hour delay out of the box followed before the four minute test phase in the box with third copies of each object from sample phases 1 and 2.



Figure 4: The Prefrontal Cortex-dependent Temporal Order Recognition Task. The top, middle, and bottom boxes show the apparatus in Sample Phase 1, Sample Phase 2, and the Test Phase, respectively, of the testing portion of the protocol. There was a 1 hour delay following the first sample phase and a 3 hour delay following the second sample phase.

Fixation, Tissue Sectioning, and Tissue Sampling

Rats were euthanized via IP injection of fatal plus, followed by an ascending aorta, perfusion of 300ml of saline followed by 600 ml of 4% PFA. The brains were post-fixed in PFA for a day, then cryoprotected in a mixture of 4% PFA and 30% sucrose for another day prior to extraction. Sections were cut on a microtome at 40 μm and were placed into well trays with 0.01% Sodium Azide in phosphate buffered saline (PBS; pH 7.4) until tissue processing.

Every 9th tissue section was selected from the original series for each rat and was Nissl stained in order to standardize the location between rats within the hippocampus. Tissue sections were compared to sections from the Paxinos & Watson Brain Atlas. After selecting the range to be analyzed for each rat, sixteen tissue sections were randomly selected within the desired hippocampal range, anterior-to-posterior locations corresponding to Bregma -2.76mm to -4.36mm, a range from Figures 56-69, in the Paxinos Atlas.

Immunohistochemistry

The sixteen sections within the chosen Paxinos and Watson Brain Atlas (Paxinos and Watson) range for each rat were separated into 4 groups and mounted onto gel-coated slides. The sections were then immunohistochemically stained for

parvalbumin (PV), somatostatin (SOM), neuropeptide Y (NPY), and calbindin (CB). SOM was co-labeled with NPY because both are neuropeptides, and PV and CB were co-labeled because both are calcium binding proteins. One of the four tissue section groups was reserved for further Nissl standardization, and one was set aside for co-labeling of calretinin (CR) and VIP interneuron biochemical markers, to be analyzed in future studies.

The initial step of the immunohistochemistry procedures included the blocking of all tissues with Goat Serum for low-affinity, non-specific binding of antigens. The slides were placed in a solution of Phosphate Buffer Saline (PBS), 3% Goat Serum, and 0.25% Triton X, then incubated for 24 hours on a shaker set at 60 rpm.

The following day, the slides were separated based on the interneuron type for which each was selected to be stained. The slides were then transferred to solutions of primary antibodies against the respective interneuron biochemical markers: 100 μ L Monoclonal Anti-Parvalbumin antibody produced in mouse (Sigma-Aldrich product number P3088), 50 μ L Anti-Calbindin antibody produced in rabbit (Abcam product number ab11426), 200 μ L Anti-Somatostatin antibody produced in mouse (Santa Cruz product number sc-74556), and 200 μ L Anti-Neuropeptide Y (NPY) antibody produced in rabbit (Sigma-Aldrich product number N9528). The calcium binding protein primary antibodies were diluted to concentrations of 1:2000 and the neuropeptide primary antibodies were diluted to 1:1000 concentrations.

Secondary antibody staining was completed on the third day of the immunohistochemistry process. Prior to the staining, the tissues were washed three times in PBS for five, ten, and 45 minute durations. The slides were then placed in a solution containing 198.7 mL PBS and 200 μ L of each fluorescently-tagged secondary antibody, diluted to a concentration of 1:500 dilution of 200 mL for both the Alexa Fluor 594 Goat Anti-Rabbit IgG and Alexa Fluor 488 Goat Anti-mouse IgG. The slides were covered with foil, in order to protect the fluorescence from light, and placed on the shaker for 48 hours at 60 rpm.

On the fourth day, the slides underwent three 15-minute washes in PBS with a foil covering protecting them from light. The dried slides were coverslipped in Vectashield mounting medium with Dapi (produce number H-1200).

Fluorescent Microscopy

Images were taken using a 20x air objective on the DeltaVision RT Deconvolution Microscope. Six randomly selected areas were chosen for imaging within each of the three regions of interest: CA1, CA3, and Dentate Gyrus (Figure 5). Three images each were taken from CA1 Stratum Oriens, CA1 Stratum Radiatum, CA3 Stratum Oriens, CA3 Stratum Radiatum, dentate granule cell layer, and dentate hilus.

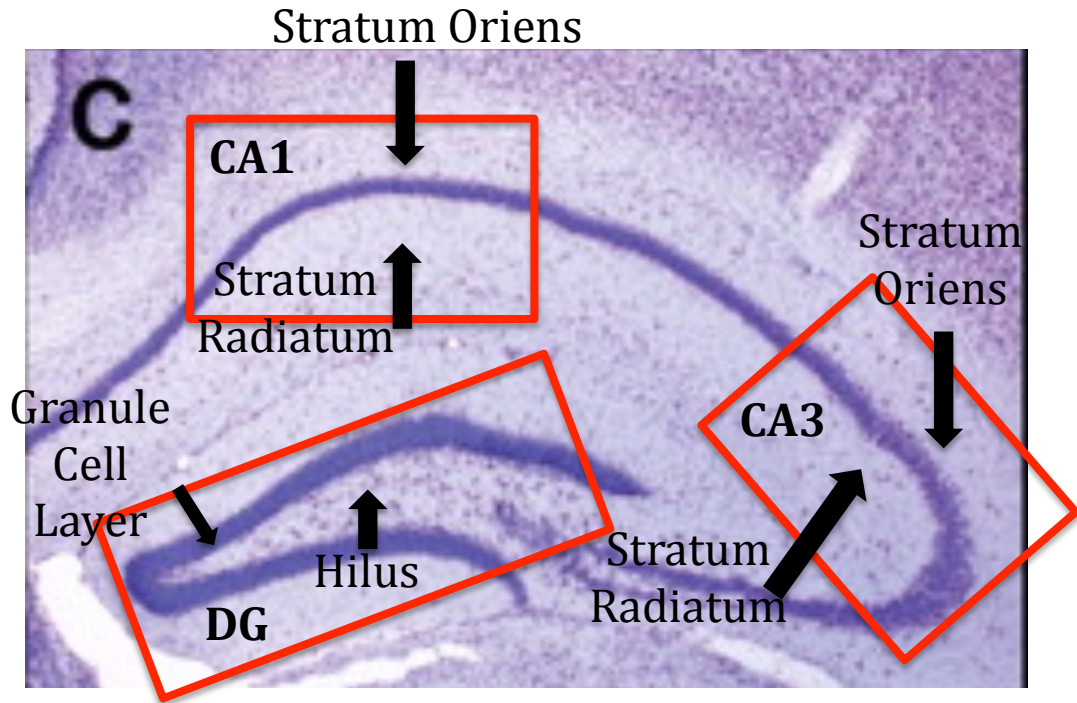


Figure 5: Immunofluorescent Imaging. The Paxinos & Watson Brain Atlas Nissl stain above shows the regions of the hippocampus from which imaged samples were taken. Red boxes indicate regions and the arrows show the respective layers within the hippocampus that images were taken.

Image Acquisition and Quantification

An optical fractionation approach was used in quantifying interneuron densities to avoid the effects of fragmented cells at the edges of the tissue. In all samples acquired, the center of the tissue was determined by the experimenter, then 15 microns surrounding this center was acquired in the z-plane of the tissue. Since the x and y dimensions of the tissue were always constant, this 15 micron z-sampling ensured that every sample was composed of the same volume, thus facilitating comparisons between different sections from different animals.

Quantification and Statistical Analysis

After acquisition, all images were imported into Adobe Photoshop where they were line averaged. Cells were counted by a separate observer who was blind to the identity of the animals, and was also different from the experimenters who acquired the images. In accordance with previously described sampling techniques, all neurons falling within the image boundaries and touching two randomly chosen edges of the sample were counted. An immunoreactive cell was identified as having immunoreactivity to the various markers and a punctate, cellular morphology (Images 1, 2, 3, and 4). Counts were combined for every antibody-region combination in every animal, and statistics were performed at the single animal level. A two-way ANOVA with a significance criterion of $p < 0.01$ was used for all age comparisons.

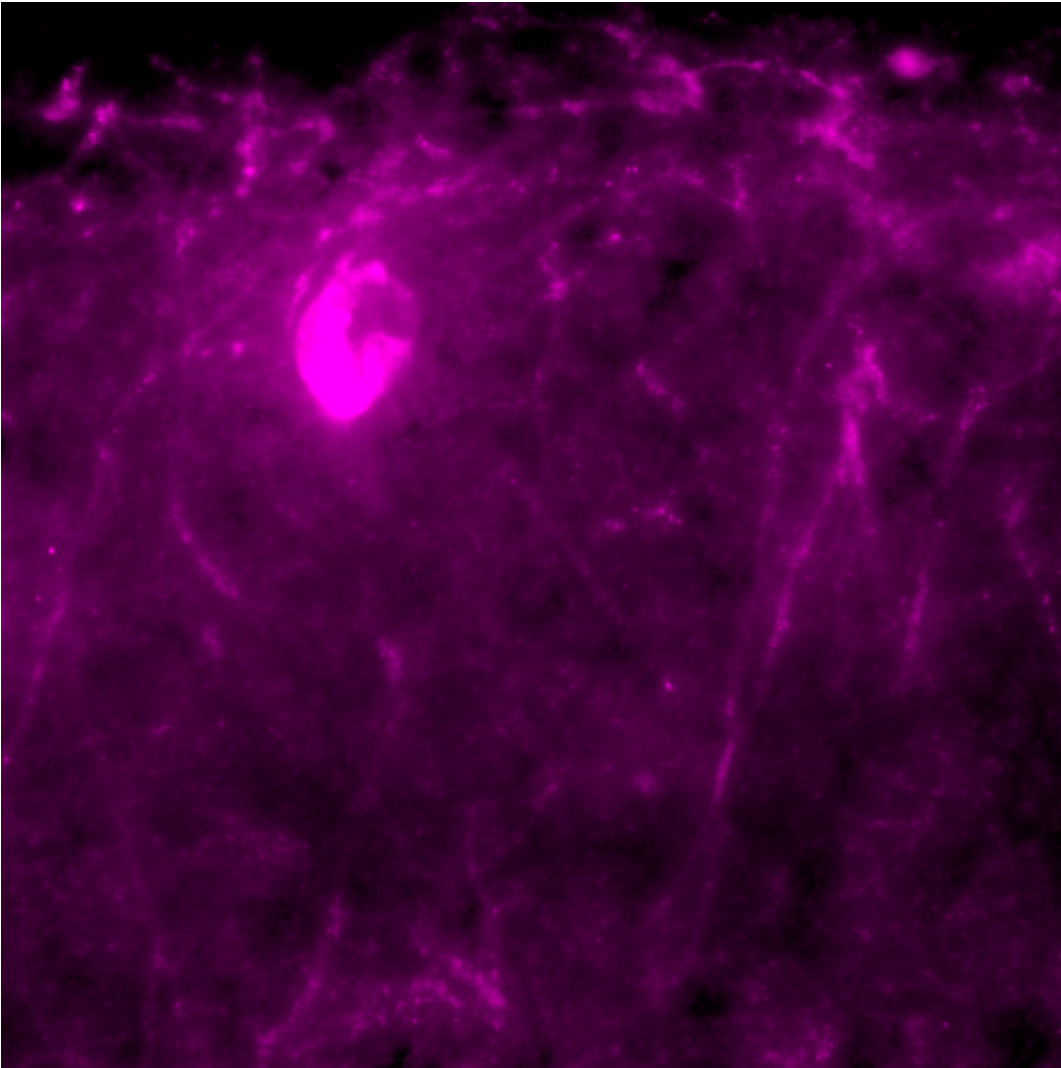


Image 1: PV-immunoreactive neurons in CA1 stratum oriens.

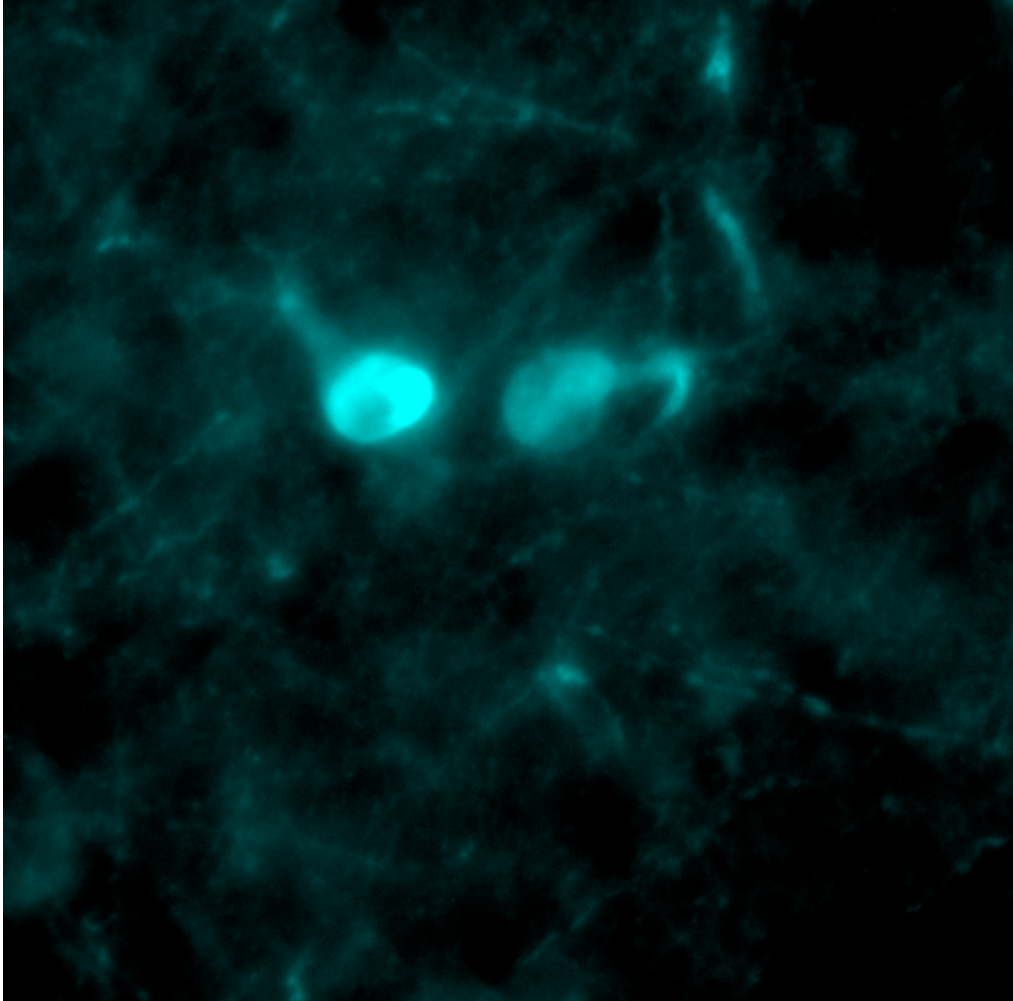


Image 2: CB-immunoreactive neurons in CA3 stratum radiatum.

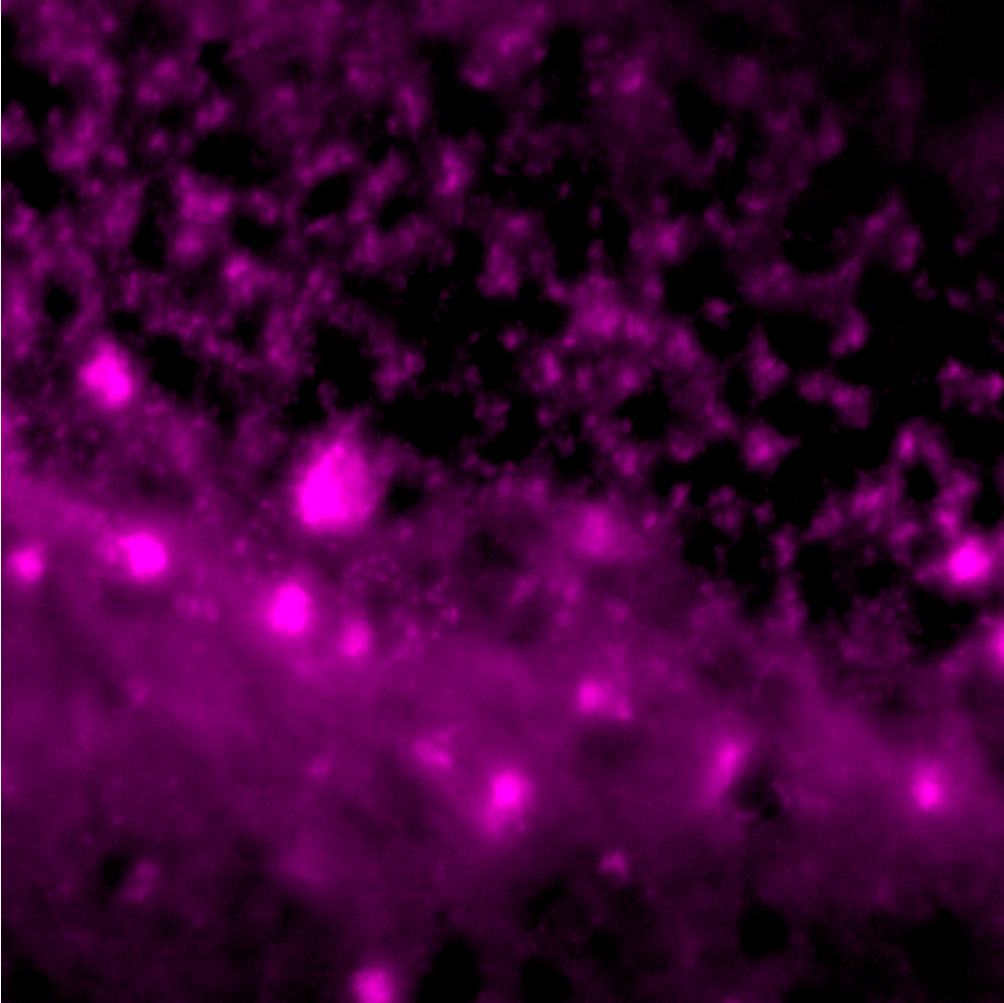


Image 3: SOM-immunoreactive neurons in DG granule cell layer.

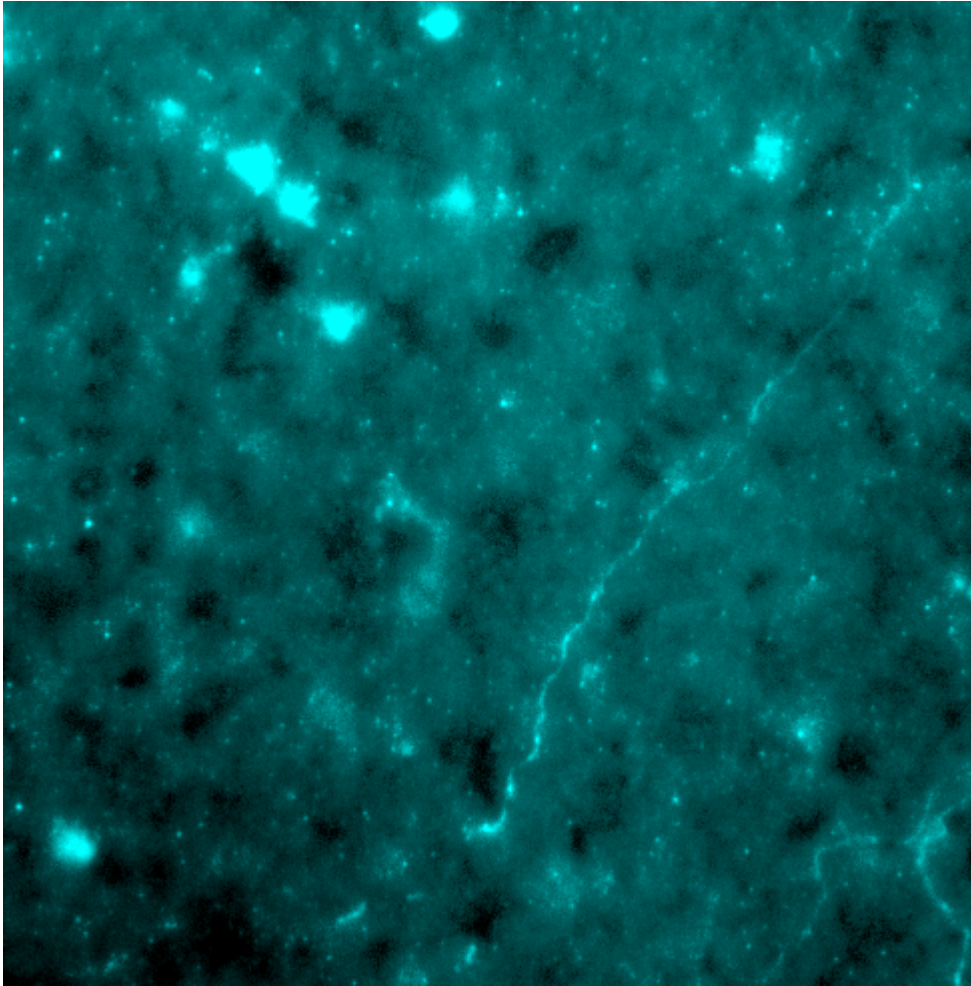


Image 4: NPY-immunoreactive neurons in CA3 Stratum Radiatum.

Results

Behavioral

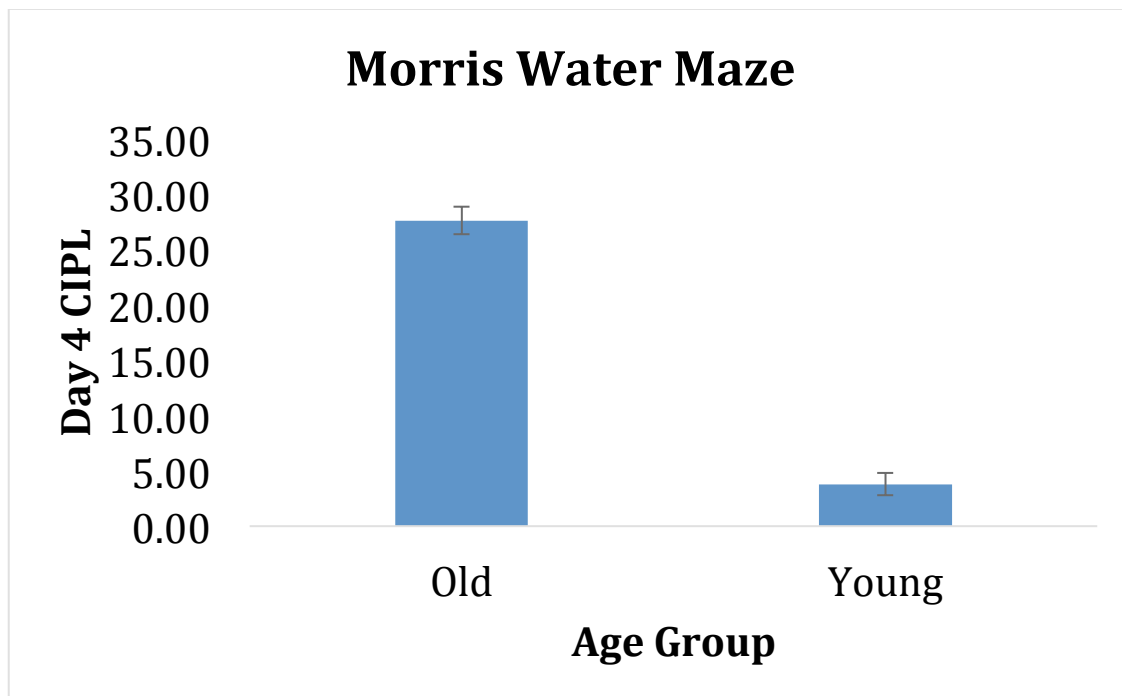
This population of aged rats showed significant decreases in performance compared to the younger rats in both of the hippocampus-dependent tasks, the Morris Watermaze and the inbound W-track task (Graph 1 and Table 2). However, there were no significant age-related differences in performance of the prefrontal cortex-dependent tasks, the SOR, TOR, and outbound W-track tasks (Graph 2, 3, and Table 2). The lack of an age-related effect in the SOR and TOR tasks came as a surprise as this laboratory has shown multiple times that aged rats are impaired on these tasks. One possibility is that the behavioral battery in the current study placed these two tasks after the watermaze and the w-maze. It is conceivable that the extensive training on the first two behavioral tasks could have rescued some of the behavioral impairments in the aged animals.

Histological: Interneuron Population Cell Densities

In the dentate granule cell layer there was a significant increase in the density of SOM-expressing interneurons within the aged rats ($p < 0.01$; two-way ANOVA). Old rats had an average of 5.726 ± 0.366 cells per image, while the younger rats had a mean of 4.245 ± 0.285 SOM-immunoreactive interneurons counted per image (Graph 4). There was no change observed in any of the other three interneuron population densities expressing CB, PV, or NPY in the dentate granule cell layer.

In the dentate hilus, NPY was shown to significantly increase ($p < 0.01$; two-way ANOVA). Aged rats had an average of 9.043 ± 0.715 NPY-immunoreactive interneurons counted in each image, while the young rats had an average of 5.867 ± 0.484 NPY-immunoreactive cells per image (Graph 5). There were no significant changes in SOM, CB, or PV-expressing interneuron densities in the dentate hilus. While these data indicate density increases, this does not necessarily mean an increase in total cell number, as tissue shrinkage is a possibility. Decreases in the volume of the hippocampus could effectively compress the existing cells and yield a density estimation that is higher. Thus, a volumetric analysis of the hippocampus is necessary for a precise stereological estimate of cell number. These data are currently being prepared.

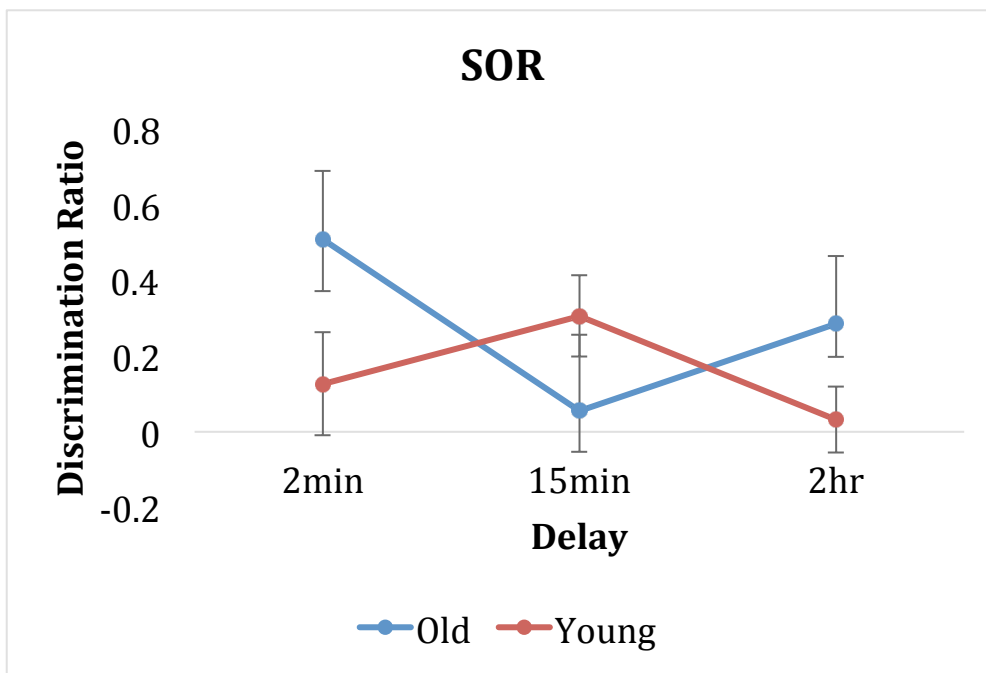
The results showed no changes in SOM, PV, CB, or NPY-expressing interneuron densities in either of the analyzed sub regions of the CA1 or the CA3 (Graphs 6-9).



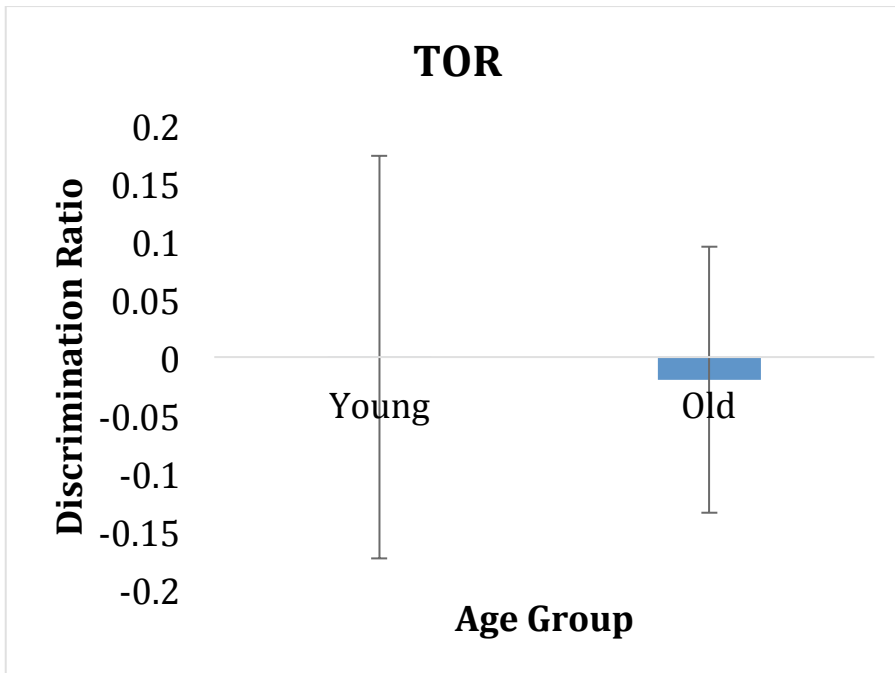
Graph 1: Morris Watermaze Results. Older animals had significantly higher corrected integrated path lengths (CIPL), or total distances from the target throughout the final day of training, signifying worse spatial memory performance.

W-MAZE	Average # Trials IN	Average # Trials OUT	Proportion Correct IN	Proportion Correct OUT	Proportion of Side-to-side Errors
Young	291	314	0.90	0.59	0.08
Old	119	114	0.75	0.54	0.20
<i>t</i> -test p-value <	0.0001	0.000009	0.004	0.23	0.003

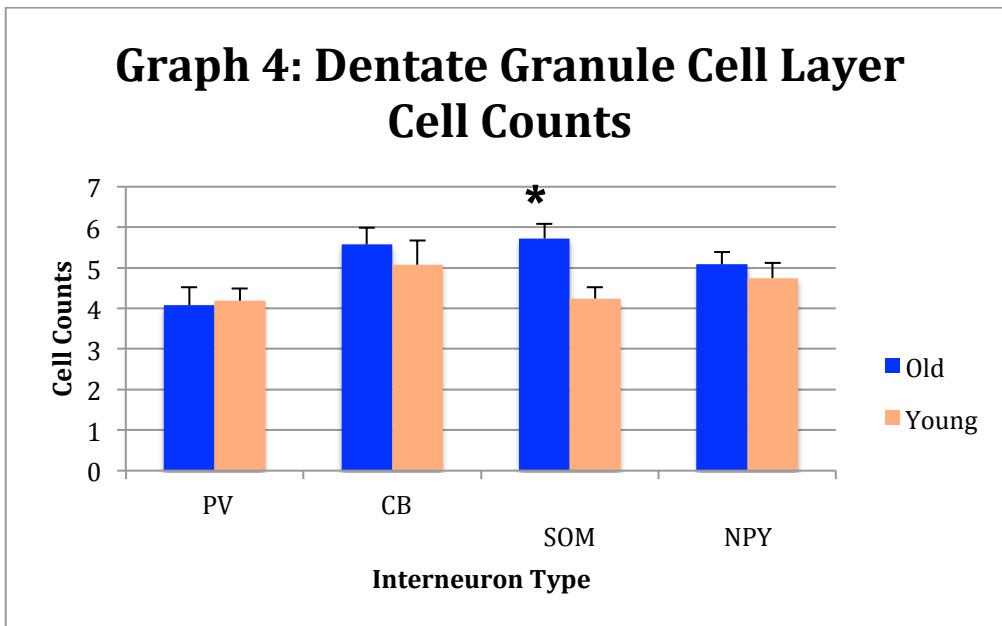
Table 2: W-Maze Continuous Spatial Alternation Task Results. Older animals performed fewer trials (ran less), were worse on inbound paths (70% compared to 90%, $p < 0.004$), had no statistical difference on outbound paths, and made a higher percentage of side-to-side errors compared to young (20% compared to 8%, $p < 0.003$).



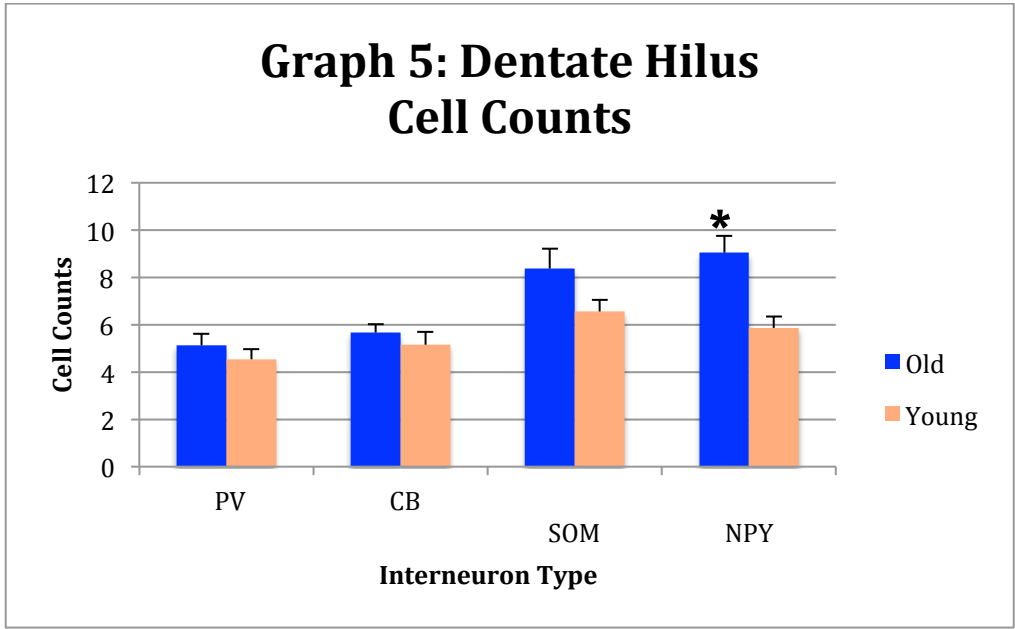
Graph 2: SOR Results. There was substantial variance and thus no statistically significant differences in the discrimination ratios of novel and familiar objects between young and old rats.



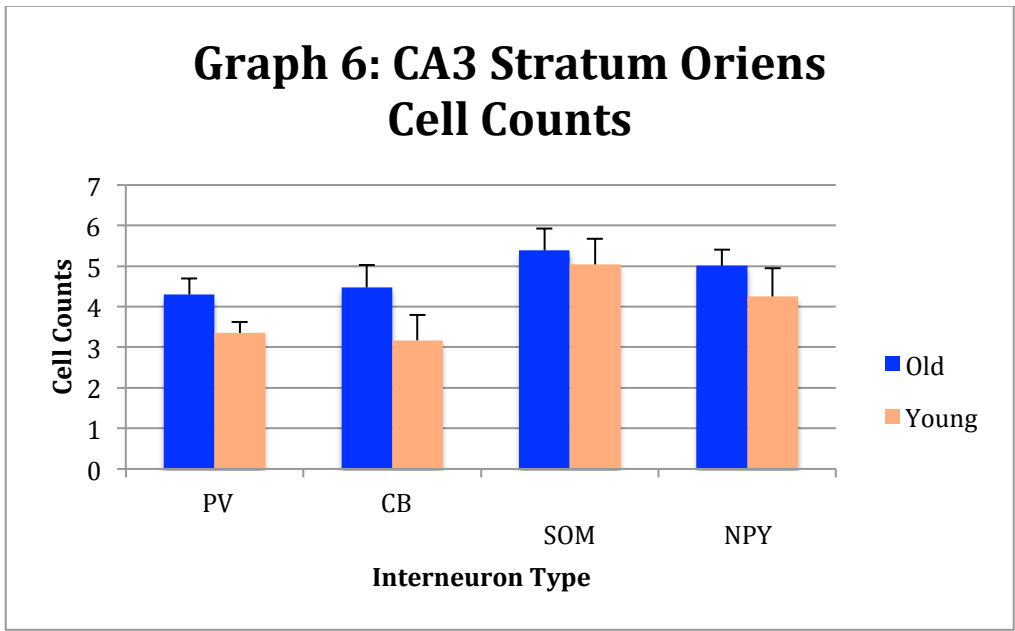
Graph 3: TOR Results. There were no statistically significant differences in the discrimination ratios of novel and familiar objects between young and old rats.



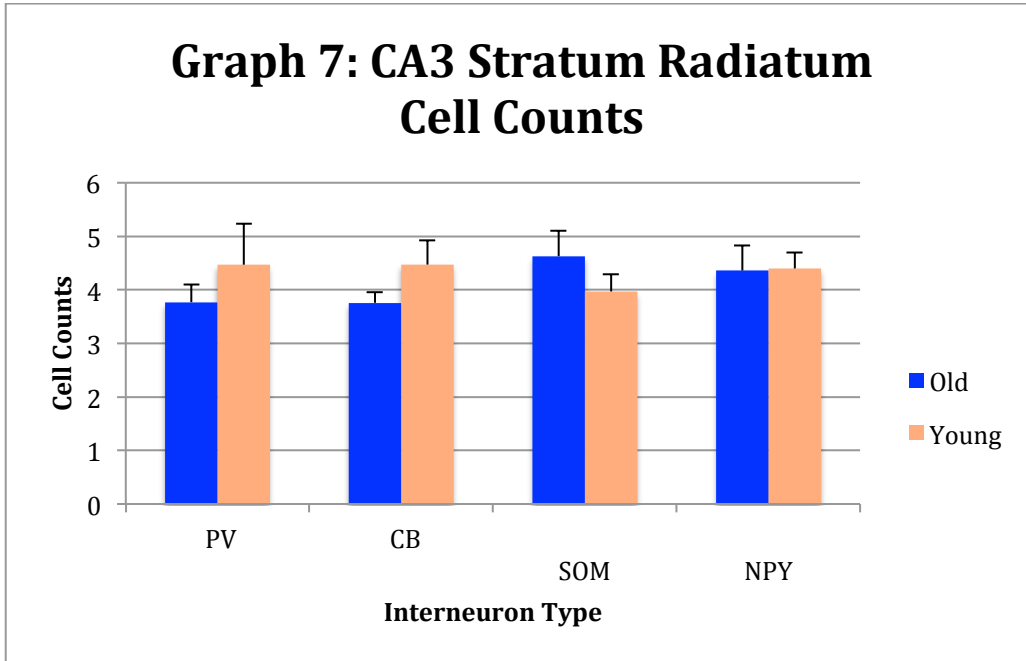
Graph 4: Cell counts in the Granule Cell Layer of the Dentate Gyrus. There were no differences in the PV, CB, and NPY cell counts between young and old rats. However, there was a significant increase in the numbers of SOM-immunoreactive cells of old rats.



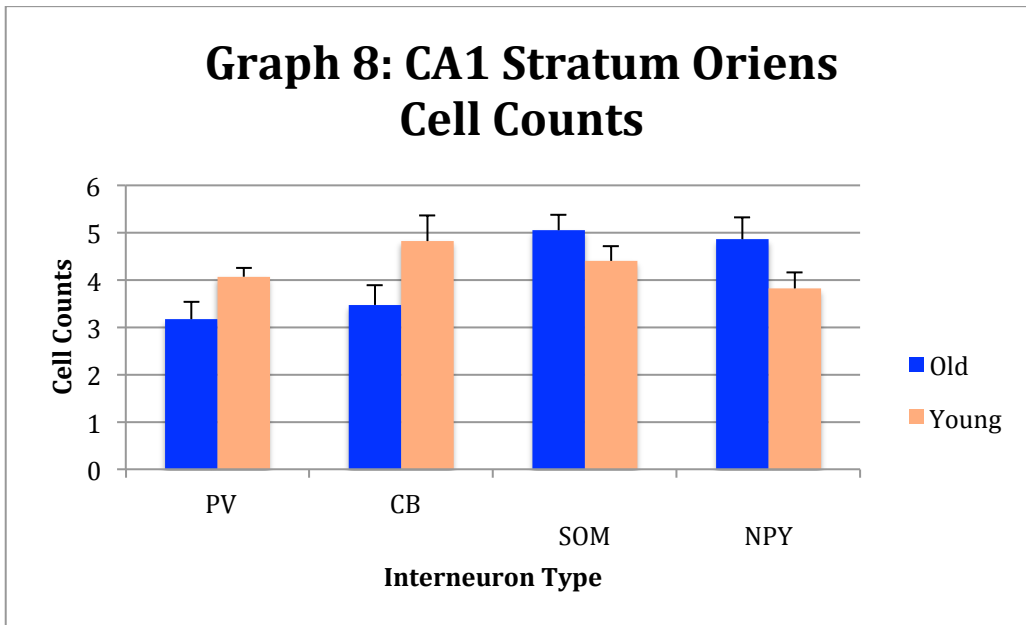
Graph 5: Cell counts in the Hilus of the Dentate Gyrus. There were no differences in the PV, CB, and SOM cell counts between young and old rats. However, there was a significant increase in the numbers of NPY-immunoreactive cells of old rats.



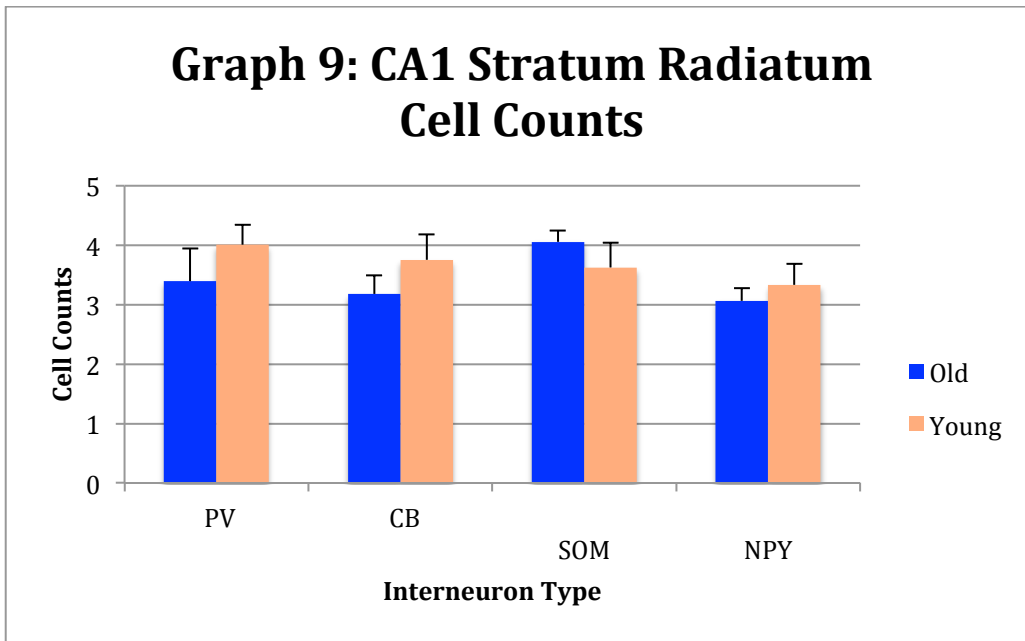
Graph 6: Cell counts in Stratum Oriens of CA3. There were no statistically significant differences in the PV, CB, SOM, and NPY cell counts between young and old rats.



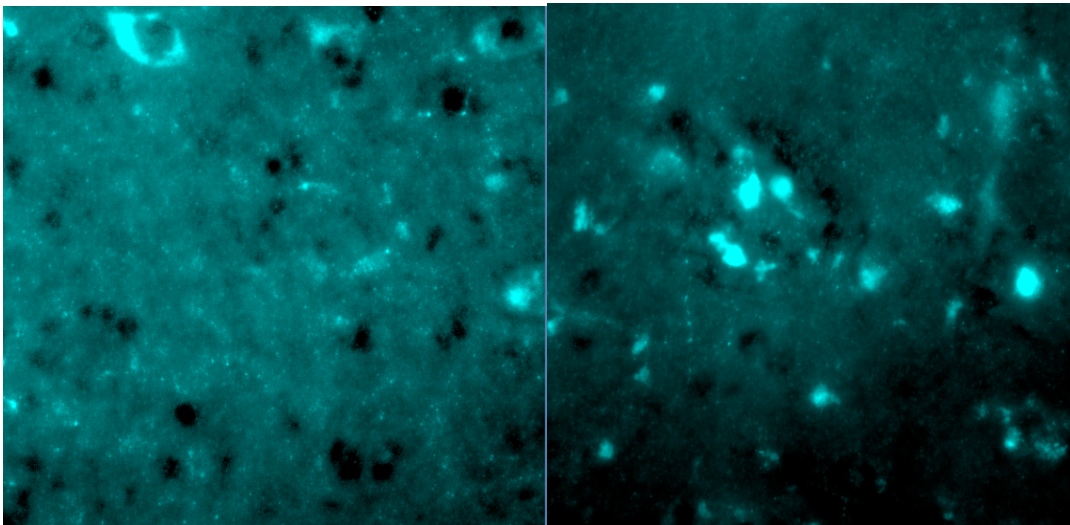
Graph 7: Cell counts in Stratum Radiatum of CA3. There were no statistically significant differences in the PV, CB, SOM, and NPY cell counts between young and old rats.



Graph 8: Cell counts in Stratum Oriens of CA1. There were no statistically significant differences in the PV, CB, SOM, and NPY cell counts between young and old rats.



Graph 9: Cell counts in Stratum Radiatum of CA1. There were no statistically significant differences in the PV, CB, SOM, and NPY cell counts between young and old rats.



Images 5 & 6: To demonstrate what an increase in cell count looks like, above is a comparison between the NPY-immunoreactive cells in the DG hilus of a young rat beside those of an old rat. The left image is from the young rat and the right is from the old rat, which visibly contains more NPY fluorescence.

Discussion

Aged rats typically show decreases in performance on prefrontal cortex-dependent behavioral tasks. In this study, however, aged rats did not show a decrease in performance of the prefrontal cortex-dependent tasks, while a decrease

was observed in the hippocampal-dependent tasks in the aged rats. The hippocampal-mediated tasks were performed first, and required rigorous training. Thus, it is possible that the older rats in this study somehow benefited from this extensive training experience, so that by the time they moved on to the second set of tasks, that were sensitive to the prefrontal cortex function, the benefit of this training led to increased performance. We would need to do a direct test of this hypothesis, however, to evaluate whether this idea was valid.

Even more unexpected were the interneuron cell density findings. Although varied results of interneuron expression and densities have been found in previous research, calbindin-expressing interneurons have never been reported to be preserved in the CA1 of the aged rat hippocampus, and always showed decreases in expression with aging (Potier et al., 2006). Likewise, somatostatin-expressing interneuron densities have also consistently shown a decrease in both the CA1 and the CA3 (Spiegel et al., 2013), and have never previously been reported to be preserved in any area of the hippocampus of the aged rat. Both were shown to be preserved in the current study.

The most surprising of our findings was the increase in somatostatin expressing interneurons in the dentate granule cell layer, and the increase in NPY in the dentate hilus. In fact, somatostatin and NPY expressing interneuron densities both, have exclusively been shown to decrease in both the dentate granule cells and dentate hilus (Cadacio et al., 2003; Hattiangady et al., 2005; Spiegel et al., 2013).

When looking for potential explanations for our unexpected findings, the major difference between our study and others is the extensive behavioral tests that the rats performed. Not only did we do behavior tests, but four tasks were administered to each of the 12 rats.

Possible explanations for the differences in interneuron expressions in the results of this study may be loosely related to changes in chemical expression in the interneurons rather than interneuron degradation. We draw support for this hypothesis from findings that interneurons undergo phenotypic changes in the hippocampus (Stanley and Shetty, 2004).

Another possible explanation for these results may be due to the fact that both young and old rats in this study were exposed to physical activity, including excessive amounts of running, which has been shown to double the amount of surviving newborn cells in the hippocampus (Praag et al., 1999). Therefore, since we found SOM and NPY-expression increases localized to the dentate gyrus, neurogenesis has to be considered. Neurogenesis in the hippocampus takes place throughout the adult life (Aberg et al., 2000) and is highly responsive to hippocampus-dependent learning tasks (Cao et al., 2004). Neurogenesis in older rats has been shown to correlate with worse performance on learning and memory tasks (Bizon and Gallagher, 2003), which we did see evidence of in the hippocampal dependent Morris Watermaze and W-track.

One cause for neurogenesis in the aged rat more so than the young rat could be related to compensation of reduced dendritic branching. Dendrites in pyramidal and granule hippocampal cells in the aged rat exhibit short, thick, and poorly branched processes compared to the younger adults who display long, extensively branched processes (Lolova, 1992). The higher population of hippocampal cells in

the aged rat could possibly serve as a compensatory mechanism for the lack of branching when faced with the learning of new behavioral tasks.

A third, less supported argument for the increase in expression in the dentate gyrus of the aged rat could be related to stress levels induced by the behavior testing. The Morris Watermaze is often used when testing for stress factors and is known to increase stress levels in rats. This is important because memory is impaired when accompanied by an increase in corticosterone levels (de Kloet et al., 1999). The poor performance of the aged rats could have been related to increased stress levels, which are known to inhibit neurogenesis in the hippocampus. These effects can be reversed once the cortisol level decreases, resulting in a rebound of increased numbers of new cells (Cameron and McKay, 1999). Other less stressful tests of spatial memory also show age-related memory impairments, which makes stress unlikely to be the only contributor to these deficits.

Despite the fact that densities were preserved in most of the interneurons, we still saw a decrease in hippocampal dependent behavior tasks in the aged rats, which may indicate that conclusions about behavior cannot be drawn from SOM, CB, PV, or NPY-expressing interneuron densities. Future studies may look closer at behavioral tasks by using only one or two behaviors per cohort to see if more specific conclusions can be drawn.

Acknowledgements

We would like to thank the Barnes Laboratory technicians, Ajay Upretty and Arturo Espinoza, and the undergraduate research assistants, Adele Koutia, Anastasia Zavilla, and Allison Comrie, for their assistance in the animal care and behavioral testing of the animal subjects in this study.

References

Aberg, M., Aberg, D., Hedbacker, H., Oscarsson, J., Eriksson, P., (2000) Periferal infusion of IGF-I selectively induces Neurogenesis in the adult rat hippocampus. *Journal of Neurosci.* 20:8, 2896-2903.

Bizon, J.L., Gallagher, M., (2003) Production of new cells in the rat dentate gyrus over the lifespan: relation to cognitive decline. *European Jour. of Neurosci.* 18:1, 215-219

Cadacio, C.L., (2003) Hilar neuropeptide Y interneuron loss in the aged rat hippocampal formation. *Exp Neurology.* 183:1, 147-158.

Cameron, H.A, McKay, R.D.G., (1999) Restoring production of hippocampal neurons in old age. *Nature Neuroscience.* 2, 894 – 897.

Chan-Palay, V. (1991) Somatostatin immunoreactive neurons in the human hippocampus and cortex shown by immunogold/silver intensification on vibratome sections: coexistence with neuropeptide Y neurons, and effects in Alzheimer-type dementia. *Jour of Comp Neurology*. 260:2, 201-123.

Cao, L., Jiao, X., Zuzga, D., Lui, Y., Fong, D., Young, D., During, M., (2004) VEGF links hippocampal activity with neurogenesis, learning and memory. *Nature Genetics*. 36:8, 827-835.

de Kloet, E.R., Oitzl, M.S., Joëls, M., (1999) Stress and cognition: are corticosteroids good or bad guys?. *Trends Neurosci*. 22, 422-426.

Dutar, P., Potier, B., Lamour, Y., Emson, P.C., Senut, M.C., (1991) Loss of Calbindin-28K Immunoreactivity in Hippocampal Slices from Aged Rats: a Role for Calcium?. *Eur J Neurosci*. 3:9, 839-849.

Freund, T. F., Buzsáki, G (1996) Interneurons of the hippocampus. *Hippocampus*. 6:4, 347-470.

Hattiangady, B., Rao, M., Shetty, G., Shetty, A., (2005) Brain-derived neurotrophic factor, phosphorylated cyclic AMP response element binding protein and neuropeptide Y decline as early as middle age in the dentate gyrus and CA1 and CA3 subfields of the hippocampus. *Exp Neurol*. 195:2, 353-371.

Kanak, D., Rose, G., Zaveri, H., Patrylo, P., (2013) Altered network timing in the CA3-CA1 circuit of hippocampal slices from aged mice. *Plos ONE*. 8:1, e61364.

Koh, M., Haberman, R., Foti, S., McCown, T., Gallagher, M., (2010) Treatment strategies targeting excess hippocampal activity benefit aged rats with cognitive impairment. *Neuropsychopharmacology*. 35:4, 1016-1025.

Koh, M., Rosenzweig-Lipson, S., Gallagher, M., Selective GABA(A) $\alpha 5$ positive allosteric modulators improve cognitive function in aged rats with memory impairment. *Neuropsychopharmacology*. 64. 145-152.

Kuruba, R., Hattiangady, B., Parihar, V., Shuai, B., Shetty, A., Differential susceptibility of interneurons expressing neuropeptide Y or parvalbumin in the aged hippocampus to acute seizure activity. *Plos ONE*. 6:9, e24493.

Lolova, Ivanka, (1992) Age-related morphological and morphometrical changes in parvalbumin- and calbindin-immunoreactive neurons in the rat hippocampal formation. *Mech Ageing Dev*. 66:2, 195-211.

Lu, C., Hamilton, J., Powell, A., Toescu, E., Vreugdenhil, M., (2011) Effect of ageing on CA3 interneuron sAHP and gamma oscillations is activity-dependent. *Neurobiol. Ageing*. 32:5, 956-965.

Maei, H., Zaslavsky, K., Teixeira, C., Frankland, P., (2009) What is the most sensitive measure of water maze probe test performance?. *Front Interg Neorosci*. 3, 4.

Mitchell, J., Sundberg, K., Reynolds, J., (2007) Differential attention-dependent response modulation across cell classes in macaque visual area V4. *Neuron*. 55:1, 131-141.

Myers, C., Scharfman, H., (2009) A role for hilar cells in pattern separation in the dentate gyrus: a computational approach. *Hippocampus*. 19:4, 321-337.

Paxinos, George, and Charles Watson. *The Rat Brain, in Stereotaxic Coordinates*. 7th ed. San Diego: Academic, 2014. Print.

Potier, B., Jouvenceau, A., Epelbaum, J., Dutar, P., (2006) Age-related alterations of GABAergic input to CA1 pyramidal neurons and its control by nicotinic acetylcholine receptors in rat hippocampus. *Neuroscience*. 142:1, 187-201.

Potier, B., Krzywkowski, P., Lamour, Y., Dutar, P., (1994) Loss of calbindin-immunoreactivity in CA1 hippocampal stratum radiatum and stratum lacunosum-moleculare interneurons in the aged rat. *Brain Research*. 661:1-2, 181-188.

Praag, H., Kempermann, G., (1999) Running increases cell proliferation and neurogenesis in the adult mouse dentate gyrus. *Nature Neurosci*. 2:3, 266-270.

Rapp, P., Gallagher, M., (1996) Preserved neuron number in the hippocampus of aged rats with spatial learning deficits. *Proc. Natl. Acad. Sci. U.S.A.* 93:18, 9926-9930.

Rapp, P., Deroche, P., Mao, Y., Burwell, R., (2002) Neuron number in the parahippocampal region is preserved in aged rats with spatial learning deficits. *Cereb Cortex*. 12:11, 1171-1179.

Roberts, G. W., Crow, T. J., Polak, J. M., (1985) Location of neuronal tangles in somatostatin neurones in Alzheimer's disease. *Nature*. 314:6006, 92-94.

Shetty, A., Turner, D., (1998) Hippocampal interneurons expressing glutamic acid decarboxylase and calcium-binding proteins decrease with aging in Fischer 344 rats. *J. Comp. Neurol*. 394:2, 252-269.

Shi, L., Argenta, A., Winseck, A., Brunso-Bechtold, J., (2004) Stereological quantification of GAD-67-immunoreactive neurons and boutons in the hippocampus of middle-aged and old Fischer 344 x Brown Norway rats. *J. Comp. Neurol*. 478:3, 282-291.

Singec, I., Knoth, R., Ditter, M., Volk, B., Frotscher, M., (2004) Neurogranin is expressed by principal cells but not interneurons in the rodent and monkey neocortex and hippocampus. *J. Comp. Neurol.* 479:1 30-42.

Spiegel, A., Koh, M., Vogt, N., Rapp, P., Gallagher, M., (2013) Hilar interneuron vulnerability distinguishes aged rats with memory impairment. *J. Comp. Neurol.* 521:15, 3508-3523.

Stanley, D., Shetty, A., (2004) Aging in the rat hippocampus is associated with widespread reductions in the number of glutamate decarboxylase-67 positive interneurons but not interneuron degeneration. *J. Neurochem.* 89:1, 204-216.

Stanley, E., Fadel, J., Mott, D., (2012) Interneuron loss reduces dendritic inhibition and GABA release in hippocampus of aged rats. *Neurobiol. Aging.* 33:2, 431.e1-13.
Thome A, Gray DT, Erikson CA, Lipa P, Barnes CA (2015).

Thome A, Gray DT, Erikson CA, Lipa P, Barnes CA (2015). Memory impairment in aged primates is associated with region-specific network dysfunction. *J Neurosci* (Under Review).

van de Nes, J. A. P., Sandmann-Keil, D., Braak, H., (2002) Interstitial cells subjacent to the entorhinal region expressing somatostatin-28 immunoreactivity are susceptible to development of Alzheimer's disease-related cytoskeletal changes. *Acta Neuropathol.* 104:4, 351-356.

Vela, J., Gutierrez, A., Vitorica, J., Ruano, D., (2003) Rat hippocampal GABAergic molecular markers are differentially affected by ageing. *J. Neurochem.* 85:2, 368-377.

Wilson IA, Ikonen S, Gallagher M, Eichenbaum H, Tanila H (2005). Age-associated alterations of hippocampal place cells are subregion specific. *J Neurosci* 25: 6877–6886.

Yassa, M.A., Stark, S.M., Bakker, A., Albert, M., Gallagher, M., Stark C.E., (2011) High resolution structural and functional MRI of hippocampal CA3 and dentate gyrus in patients with amnesic mild cognitive impairment. *Neuroimage.* 51, 1242-1252.

Yassa, M.A., Lacy, J.W., Stark, S.M., Albert, M., Gallagher, M., Stark C.E. (2011) Pattern separation deficits associated with increased hippocampal CA3 and dentate gyrus in non-demented older adults. *Hippocampus.* 21, 968-979.

STUDY	SPECIES: Strain	AGE & SAMPLE SIZE	REGION: Layer	INTERNEURON TYPE	IHC: Marker	BEHAVIOR	PHYSIOLOGY	RESULTS	NOTES
Cadacio et al. (2003)	Male Long Evans Rats	Young= 6mo (n=11); Aged= 24-28mo (n=2)	Dentate Gyrus	NPY-I interneurons	1:6000 dilution of anti-NPY. 1:400 dilution of goat anti-rabbit immunoglobulin (IgG) conjugated to biotin, peroxidase-avidin complex	Morris Watermaze	N/A	Reduction in number of hilar NPY-I interneurons associated with aging, but not spatial learning impairment.	Immunolesioning of the cholinergic septohippocampal pathway resulted in a selective reduction in the number of hilar NPY-I interneurons to 73% of control values on average. A subgroup of these interneurons may be dependent on neurotrophic support derived from cholinergic afferents.
Chan-Palay (1987)	Human	Non-postmortem tissue from 12 neocortices of patients who underwent surgery primarily for large brain tumors or for intractable temporal lobe epilepsy. 3 cases of severe Alzheimer's Type Dementia (ATD) & 3 controls matched for age, 3 young male controls	Hippocampal formation, retrohippocampal region, and temporal cortex	SOM& NPY	Primary antisera that recognize somatostatin-14 or somatostatin-28, polyclonal somatostatin-14 affinity-purified (Dr. L.T. Lin) and polyclonal SOM-14 tyrosine (Immunonuclear Corp., USA, and Milab, Sweden), and four polyclonal SOM-28 antisera (Peninsula Lab. and Immunonuclear Corp., USA, and Prof. J. Potkin). Polyclonal anti-NPY raised in rabbits against unconjugated porcine NPY (Cambridge UK lot #1086)	N/A	N/A	Hippocampi and temporal cortices in cases of Alzheimer-type dementia compared to those of age-matched control brains, there is a significant to severe loss of somatostatin immunoreactive neurons and axons. This loss is most severe in those regions with the highest indices of neurofibrillary tangles and neuritic plaques—the hilus of the area dentata, CA1, and the entorhinal and perirhinal cortices. Surviving somatostatin neurons are distorted with short dendrites and truncated axons. Somatostatin-NPY coexistence is particularly high in the hilus of the area dentata, the subicular complex, and the deep layers of the entorhinal and perirhinal cortices. There is equally severe destruction of both peptide neurons in the area dentata and CA1, although more NPY neurons and networks survive in the cortices than SOMI neurons.	Diseased hippocampi were selected for (a) severity of their clinical conditions, (b) the high counts of neuritic plaques and neurofibrillary tangles, and (c) the severity of alterations in the NPY-I neuronal circuits, which demonstrated a parallel severe loss of SOM-immunoreactive and axonal networks and serious alterations in the SOM-I innervation of these regions.
Dutar et al. (1991)	Male Sprague-Dawley Rats	Young= 4-5 mo (N = 35); Aged= 24-27mo (N=)	CA1 & CA2	CaBP-positive pyramidal cells	1/4000 concentration polyclonal antiserum directed against CaBP-28k	N/A	Excitatory and inhibitory postsynaptic potentials (EPSPs/IPSPs) were induced using bipolar electrodes positioned in the stratum radiatum to activate Schaffer collaterals/commissural fibres. LTP was elicited by applying two brief (1 s), high-frequency (100 Hz) stimulus trains (separated by 20s) to Schaffer collaterals. → Long-term potentiation (LTP) of hippocampal slices failed to show significant changes in CaBP immunoreactivity, suggesting that this calcium-binding protein is not directly involved in LTP processes.	Marked loss in the number of CaBP-immunoreactive pyramidal cells and interneurons in CA1 & CA2 in aged rats. CA3, CA4, and dentate gyrus showed no age-related CaBP-LI changes. No difference in the distribution pattern of CaBP-LI was observed between the dorsal and ventral hippocampal formation.	Young rats (i) the CaBP-LI was enhanced in pyramidal neurons when the slice was preincubated in a calcium-free medium, (ii) CaBP-LI was strongly decreased when the slice was preincubated in a high-calcium medium (5 mM) and when the entry of calcium into the cell was increased by a short application of an excitatory amino acid in the medium → suggesting that the loss of CaBP-LI in the hippocampus of aged rats could be due to an increase in intracellular calcium concentration
Freund and Buzsáki (1996)	N/A	N/A	Hippocampus	N/A	N/A	N/A	N/A	N/A	124-pg informative publication on hippocampal interneurons
Gavilán et al. (2007)	Male Wistar rats	Young (3–4 months), middle-aged (12 months), and aged (24–26 months); PCR analysis, young (n = 10), middle-aged (n = 5) and aged (n = 10); Youngs: acute inflammation: (i) the vehicle-injected group (n = 9) and (ii) the LPS-injected group (n = 9), chronic inflammation: (i) control animals (n = 4) injected intraperitoneally with PBS and (ii) animals injected intraperitoneally with LPS (n = 5); IHC: Young (n = 4) and aged (n = 8); Stereology: Quantified immunopositive cells for SOM in young (n = 3) and SOM and PV in aged (n = 4) rats	Hippocampus (including CA1, CA2 and CA3 subfield and dentate gyrus)	Perisomatic inhibitory PV-containing cells and the dendritic inhibitory SOM-containing cells	Mouse monoclonal antibody OX-6 (Serotec, England; 1:100), mouse monoclonal antibody against parvalbumin (PV; Swant, 1:10 000), goat-anti-mouse anti-body against somatostatin (Santa Cruz Biotechnology, Santa Cruz, CA, USA; 1:1000) and mouse monoclonal antibody against NeuN (Chemicon, Billerica, MD, USA; 1:1000)	N/A	N/A	mRNA expression of the pro-inflammatory cytokines IL-1b and tumor necrosis factor-α (TNF-α), and the iNOS enzyme was significantly increased in aged hippocampus. mRNA expression of somatostatin and somatostatin-immunopositive cell numbers decreased in aged rats compared to young and middle-aged. Hippocampal parvalbumin-containing GABAergic interneuron numbers was preserved. mRNA expression of somatostatin and IL-1b was inversely correlated in aged rats, and the decrease in somatostatin-immunopositive cells was higher in the hilus of dentate gyrus than in CA1	Principal neurons in the stratum pyramidale of hippocampus and in the granular layer of dentate gyrus. Aged animals (n = 8) did not show qualitative differences in the density of principal neurons (pyramidal cells and granular cells), compared to young animals. Unpublished data from the current demonstrated the no age-related differences in the total number of principal neurons determined by stereology in mouse hippocampus (20-month-old)
Hattiangady et al. (2005)	Fischer 344 rats	Young: 4 mo; Middle-aged: 12 mo; Aged: 24 mo	CA1, CA3, DG	Brain-derived neurotrophic factor (BDNF), transcription factor phosphorylated cyclic AMP response element binding protein (p-CREB), and neurotrophic neuropeptide Y (NPY).	Primary antibodies against BDNF (rabbit anti-BDNF, 1:100; Santa Cruz), phosphorylated form of CREB (rabbit anti-phospho-CREB, 1:100; Upstate), NPY (rabbit anti-NPY, 1:30,000; Peninsula), and NeuN (mouse anti-NeuN, 1:1000; Chemicon). BDNF was analyzed via ELISA and BDNF immunohistochemistry. p-CREB through densitometric analysis of p-CREB immunopositive cell, and NPY via stereological counting of NPY-immunopositive interneurons.	N/A	N/A	BDNF concentration, p-CREB immunoreactivity, and number of NPY immunopositive interneurons decline considerably by middle age in dentate gyrus, CA1, and CA3. p-CREB immunoreactivity diminishes further from middle to old age, but BDNF concentration and NPY immunopositive interneuron numbers exhibit no significant decrease.	CA1, CA3, DG: Reduced overall BDNF concentration, diminished BDNF immunoreactivity in the soma of neurons, decreased p-CREB immunostaining in the nucleus of neurons and decreased number of NPY immunopositive interneurons. Variable results in ELISA assays necessitate confirmation of ELISA results with immunohistochemistry → this study confirmed their ELISA results for different hippocampal regions with immunohistochemical evaluations.
Kanak et al. (2013)	Male 129/C57BL6 mice	Adult= 4.060.1mo (n=22); Aged= 21.760.3mo (n = 18)	CA3-CA1 network signaling	N/A	N/A	N/A	Field potentials were recorded using silver/silver-chloride electrodes. Juxtacellular recordings were obtained "blindly" from neurons in CA1 stratum pyramidale and stratum oriens.	The relative timing of activity in CA1 stratum pyramidale was delayed in the aged. Schaffer collateral responses were attenuated in CA3 (antidromic spike amplitude) and CA1 (orthodromic field EPSP slope). Aged neurons exhibited reduced spike probability during the early cycles of the CA3 ripple oscillation → aging disrupts the coordination of patterned activity in the CA3-CA1 circuit.	Coherent sharp wave ripples and gamma oscillations were evident in the CA3-CA1 circuit in both age groups. Aged mice amplitude and timing of spontaneous sharp waves recorded in CA1 stratum radiatum were similar to adults. The unit activity recorded juxtacellularly from unidentified neurons in CA1 stratum pyramidale and stratum oriens was temporally modulated by CA3 ripples in both age groups.
Koh et al. (2010)	Male Long-Evans Rats	Y= 6mo (LEV; n=7); Aged= 24 to 26 mo (NPA; 6 (Watermaze), LEV/6 (Watermaze), VPA; 39 (Watermaze), LEV/VPA; 10 (Radial Arm)	CA3	NPY-IR neurons	N/A, injected with either an AAV vector that expresses and constitutively secretes NPY 13–36 (targeting Y2 receptors) or control substances (AAV-GFP or saline) bilaterally into the CA3 area of the hippocampus. VPA osmotic pumps implanted subcutaneously in the intrascapular region; systemic LEV injections	Modified Morris Watermaze, Radial Arm Maze	N/A; In-Situ Hybridization; riboprobe template targeting FIB NPY 13–36 sequence	Overexpression of inhibitory NPY-13-36 in CA3 improved hippocampal-dependent, long-term memory in impaired aged rats.	2 antiepileptic drugs also improved memory → Excess CA3 activity (also seen in epilepsy) plays a role in age-related, hippocampal-dependent memory
Koh et al. (2013)	Male Long-Evans rats	Y= 6 mo; Aged rats with impaired performance but successful cued training on the Morris Watermaze= 24-26mo. GABAA a5 receptor PAM memory modulation efficacy test of Compound 44 in aged-impaired rats (n = 11). Efficacy of GABAA a5 receptor NAM in young (n = 16) & memory-impaired, not aged rats (n = 7) in a radial arm maze task. Age-impaired in Watermaze task. Compound 44 treatment (n = 6), vehicle treatment (n = 5). Compound 6 effect on young rats (n = 8) and memory-impaired, aged rats (n = 8) in radial arm maze.	CA3-DG	Principal neurons in the hippocampus (CA3 pyramidal neurons)	Compound 44 [6,6-dimethyl-3-(3-hydroxypropyl)thio-1-(thiazol-2-yl)-6,7-dihydro-2-benzothiazepine-(4H)-one] & Compound 6 [methyl 3,5-diphenylpyridazine-4-carboxylate]	Watermaze & Radial Arm Maze	N/A	Behavioral improvement was obtained with two different GABAA a5 PAMs in aged rats in the two hippocampal-dependent tasks. GABAA a5 receptor PAM, Compound 6, improved memory in the cognitively impaired aged rats, but not in young rats. The benefit observed in the radial arm maze task using Compound 6, memory-impaired aged rats showed improved spatial memory using another GABAA a5 receptor PAM, Compound 44.	Explored the use of positive allosteric modulators (PAMs), rather than NAMs, to treat excess neural activity during aging and in memory-impaired behavior characteristic of AD. Authors have conflicts of interest related to their research.
Kuruba et al. (2011)	Male F344 rats	Young adult= 5mo; Aged= 22mo. Intact young adult rats (4–5 months old; n = 5), intact aged rats (22 months old; n = 5), young adult rats receiving graded intraperitoneal injections of KA (n=6), and aged rats receiving graded intraperitoneal injections of KA (n = 7).	DG, CA1, CA3	NPY & PARV-expressing interneurons	anti-NPY antibody (1:1000, Peninsula laboratories, San Carlos, CA) incubated in biotinylated goat anti-rabbit IgG (1:1000, Vector), incubated overnight in a mouse anti-parvalbumin antibody solution (1:2000 in PBS, Sigma) and treated with the biotinylated anti-mouse IgG solution (Vector).	N/A	N/A	AS (acute seizure) activity-induced TLE in old age is associated with far fewer hippocampal NPY+ and PV+ interneuron numbers than AS-induced TLE in the young adult age. NPY+ interneurons were relatively resistant to AS activity in the aged hippocampus. Whereas, PV+ interneurons were highly susceptible to AS activity in both young and old age groups.	AS activity was generated by graded intraperitoneal injections of kainic acid (KA). AS activity was terminated at three hours post-onset using diazepam injection.
Lolova and Davidoff (1992)	Male Wistar rats	Young: 3mo (n = 6); Middle-aged: 11mo (n = 5); Aged: 28mo (n = 6)	DG & CA1	PV & CaBP (Calbindin)	Monoclonal antibodies against PV and CaBP (Sigma) at a dilution of 1:1000 and 1:200, respectively. Then the sections were incubated in sequence with biotinylated antimouse IgG at 1:250 and mouse-diono PAP at 1:10.	N/A	N/A	Marked age-related changes in the morphological appearance and in the quantitative parameters characterizing the PV- immunoreactive neurons in both hippocampal regions were observed. The intensity of CaBP-immunostaining of the hippocampal principle cells and interneurons remained the same but the immunoreactive fibers were structurally altered in aging, marked atrophy and loss of PV-IR neurons, but minor changes in the appearance of CaBP-IR neurons in rat hippocampal formation in aging.	Quantitation of density, cross-sectional area, length of processes and numbers of primary processes and branches of PV-IR neurons in the dentate granule cell layer and hilus as well as in the CA1 stratum pyramidale and oriens. Higher density of PV-IR neurons in CA1 than in dentate area in 3-month-old rats. Cross-sectional neuron area and the length and number of the processes show a transient enlargement of some PV-IR neurons in 11-month-old rats. The changes in the density, size and processes of PV-IR neurons were more pronounced in the dentate area than in the CA1 area; the changes in the length and number of the processes of PV-IR neurons in pyramidal and granular layers were more pronounced than those in the oriens layer and dentate hilus.

Lu et al. (2011)	C57Bl/6 mice	Young= 3-5mo (n=10); Aged= 22-28mo (n=10)	Extracellular recordings were made from stratum radiatum of area CA3c (just outside the dentate gyrus). Whole-cell patch-clamp current recordings were made from neurons at the stratum pyramidale/stratum oriens border of CA3c.	Ca2+	Ca2+ indicator Fura-2	N/A	Whole-cell patch-clamp; Extracellular recordings	There was an age-dependent increase in the sAHP of interneurons in the presence of kainate, which may contribute to the reduced gamma oscillations in the presence of kainate and learning impairments associated with aging. Kainate-induced gamma oscillations, but not spontaneous gamma oscillations, were reduced in slices from aged mice. In contrast to young interneurons, kainate increased the medium- and slow-afterhyperpolarisation and underlying (Ca2+) transient in aged interneurons. Modulating the slow-afterhyperpolarisation by modulating L-type calcium channels with BAY K 8644 and nimodipine suppressed and potentiated, respectively, kainate-induced gamma oscillations in young slices.	Passive membrane properties, firing properties, medium- and slow-afterhyperpolarisation amplitudes, basal [Ca2+]i and firing-induced (Ca2+) transients were not different with aging. Kainate caused a larger depolarisation and increase in [Ca2+]i signal in aged interneurons than in young ones.
Maei et al. (2009)	Mice of mixed C57Bl/6N Tact1b (C57Bl/6) and 129SvEv (129) background (50:50)	6-day experiment= control data set (n= 370 probe tests) that included data from control mice in the genetic (wild-type), pharmacological (received control infusions of phosphate-buffered saline.) and neuroanatomical lesion experiments. An experimental data set (n= 388 probe tests) that included data from experimental mice in the genetic knockin mice, pharmacological, and neuroanatomical lesion experiments. 5-day protocol= wild-type mice (n= 622). A total of 1800 individual probe tests were analyzed.	Hippocampus-dependent spatial memory & learning	N/A	N/A	Watermaze	N/A	Out of the evaluation methods for performance in the Watermaze probe test, either occupancy- based (percent time in a virtual quadrant [Q] or zone [Z] centered on former platform location), error-based (mean proximity to former platform location [F]), or counting-based (platform crossings [X]) measures. P is the most appropriate measure based on P measure consistently outperformed the Q, Z, and X measures in its ability to detect group differences, regardless of sample or effect size, and using both parametric and non-parametric statistical analyses. The least popular of the four measures, proximity, was consistently more sensitive at detecting group differences.	Search accuracy in control mice peaked between 10 and 15 s, before declining), suggesting mice recognize relatively early on in the probe test that the platform is absent and shift strategy to search elsewhere. Databases were composed of probe test data that were drawn from experiments using identical apparatus, training, and probe test procedures.
Myers and Scharfman (2009)	Rats	N/A	Granule cells, mossy cells, HIPP cells, and the other inhibitory interneurons (such as basket cells and chandelier cells).	N/A	N/A	N/A	Stimulate one of select four target cells and calculate the pattern separation between it and other stimulated cells. Important values: Vest of granule cells (defines the initial "bias" of granule cells to spontaneously discharge), bINT Interneuron constant (affects the global strength of lateral surround feedback inhibition on granule cells), bHIPP HIPP cell constant (affects the global strength of HIPP inhibition on granule cells), and bMCMossy cell constant (affects the global strength of mossy cells to facilitate granule cell firing).	Adding to the literature's focus on granule cells' role in pattern separation, this model focuses on excitatory hilar mossy cells and inhibitory hilar interneurons that receive input from and project to the perforant path terminal zone (HIPP cells). Mossy cells and HIPP cells allow the system to upregulate and downregulate pattern separation in response to environmental and task demands. Specifically, pattern separation can be strongly decreased by decreasing mossy cell function and/or by increasing HIPP cell function; pattern separation can be increased by the opposite manipulations.	The model could be expanded by adding additional cell types (such as specific classes of inhibitory cell), additional connectivity to existing cell types (such as perforant path inputs to mossy and HIPP cells), and more detailed physiological characteristics (such as considering specific synapses with 5-HT1A or other receptor types). The model could also be extended to include a network representing hippocampal CA3, and allowing the two systems to interact.
Potter et al. (1994)	Srage-Dawley rats	Y= 3m A=27m (nY= 7, nA= 10 for CaBP) and (nY=8, nA= 9 for PV IHC)	Interneurons below pyramidal cell layer: Stratum radiatum and lacunosum moleculare	PV and CaBP-IR GABAergic	CaBP-28, avidin-biotin-peroxidase technique	N/A	N/A	Mean 50% of CaBP-IR interneurons reduced. 78% loss in stratum radiatum of CA1, 35% in CA3, no significant loss of PV containing interneurons	
Potter et al. (2006)	Sprague-Dawley rats	Y= 3-4m (n=4), A= 25-30m (n=4). Aged and donepezil-treated (n=4)	Pyramidal neurons in CA1 of hippocampus	GABA interneurons	Som, CB, PV, VACHT	N/A	Sharp electrode: recordings from pyramidal cells of CA1. Synaptic responses were induced by stimulation of the stratum oriens (100 S duration, intensity range 50-300 A), slow EPSPs by stimulation of cholinergic fibers in stratum oriens (repetitive 30Hz, 500 ms) Patch clamp: Miniature IPSCs performed at holding potential of -80 mV.	Nicotinic control of GABA release is lowered during aging. Selective loss of subpopulations of CB and SOM positive interneurons associated with general decrease in density of the cholinergic network in aged rats	
Rapp and Gallagher (1996)									
Rapp et al. (2002)**	Male Long-Evan's rats	Y= 6m (n=8), Aged= 27-28m (n= 16)	Entorhinal, perirhinal and posthinal cortices		Nissl**	Hippocampus dependent 'place' version of Morris water maze. 3x day, 8 days (60s inter-trial intervals)	N/A	Total neuron number in entorhinal, perirhinal and posthinal cortices is largely preserved during normal aging. Individual variability of hippocampal learning among the aged rats failed to correlate with neuron number in any region examined and there was no indication of selective or disproportionate loss among the aged animals with the most pronounced cognitive impairment	**Must refer to Rapp & Gallagher which I am unable to open
Roberts et al. (1985)	Human Tissue	Control: 4 males, 2 females (mean 76 yr, range 58-87yr) Alzheimer's patients: 5 male 10 female (mean 76yr, range 57-91)	Left temporal lobe: temporal cortex, amygdala, hippocampus, SOM specifically in entorhinal and temporal cortex and parahippocampal gyrus	somatostatin	Somatostatin-28, somatostatin-14, vasoactive intestinal polypeptide, cholecystokinin-octapeptide, neuropeptide-Y	N/A	N/A	A subclass of somatostatin positive neurons are affected selectively in Alzheimer's disease, these neurons also contain neuronal tangles. Destruction of somatostatin containing neurons is an early and potentially critical step in the Alzheimer's disease process.	
Shetty and Turner (1998)	Male Fischer 344	young adult = 4-6m, aged= 23-25m (n= 4/group)	stratum radiatum of CA1, the strata oriens, radiatum and pyramidale of CA3, the dentate molecular layer, and the dentate hilus	GAD, PV, CBN, and CR	GAD 67, K2 antisense, mouse PV antibody, CBN-D28k, CR antibody, avidin-biotin complex, anti-mouse IgG, anti-rabbit IgG, mouse clonop-PAP	N/A	N/A	Interneurons positive for glutamic acid decarboxylase were significantly depleted in the stratum radiatum of CA1, the strata oriens, radiatum and pyramidale of CA3, the dentate molecular layer, and the dentate hilus. Parvalbumin interneurons showed significant reductions in the strata oriens and pyramidale of CA1, the stratum radiatum of CA3, and the dentate hilus. The reductions in calbindin interneurons were more pronounced than other calcium-binding protein-positive interneurons and were highly significant in the strata oriens and radiatum of both CA1 and CA3 subfields and in the dentate hilus. Calretinin interneurons were decreased significantly in the strata oriens and radiatum of CA3 in the dentate granule cell and molecular layers, and in the dentate hilus. However, the relative ratio of parvalbumin-, calbindin-, and calretinin-positive interneurons compared with glutamic acid decarboxylase-positive interneurons remained constant with aging, suggesting actual loss of interneurons expressing calcium-binding proteins with age	
Shi et al. (2004)	Fischer 344 x Brown Norway male rats	MA= 15-17m (n=5) O=25-29m (n=5)	dorsal hippocampus: dentate gyrus, CA1, CA3	NeuN-immunoreactive (IR) cells, GAD-IR cells, and GAD-IR boutons	NeuN and 67-kDa isoform of GAD, second rabbit anti-GAD67 polyclonal antibody, horse anti-mouse IgG secondary antibody, biotinylated goat anti-rabbit IgG secondary antibody	N/A	N/A	Significant decline in GAD-IR cells between middle and old age in CA1 but not in dentate gyrus or CA3. GAD-IR boutons did not show a decline in CA1, CA3, or dentate gyrus between middle and old age. There are significantly fewer GAD-IR cells in the strata oriens, pyramidale, and radiatum of CA1 in old compared with middle-aged rats but not in any layer of CA3 or dentate gyrus. Inhibitory synaptic terminals, expressed either as GAD-IR bouton density or the ratios of GAD-IR boutons per neuron, do not show aging-associated changes in dentate gyrus, CA3, or CA1 in the present study, suggesting that GAD-IR cells, but not GAD-IR boutons, decline between middle and old age in the dorsal hippocampus and that this decline is restricted to the CA1 region of the dorsal hippocampus.	It is possible that loss of CA1 inhibitory interneurons in the dorsal hippocampus contributes to the learning and memory impairments reported in old rats.
Singec et al. (2004)	C57Bl/6 mice, Wistar rats, vervet monkeys	mice 3m (n= 20), Rats 3m (n= 5), monkeys 4yr (n=2)	granule cells of the dentate gyrus, pyramidal neurons of CA1-CA3, Monkey frontal cortex and hippocampal somatosensory cortex except layer 1	Neurogranin (NG), PV, CB, CR	polyclonal rabbit anti-NG antibody, monoclonal mouse anti-PV, monoclonal mouse anti-CB, monoclonal mouse anti-CR. Secondary: goat anti-rabbit Alexa 488, goat anti-mouse Cy3	N/A	N/A	Strong NG expression by principal cells in different neocortical layers and in the hippocampus by granule cells of the dentate gyrus and pyramidal neurons of CA1-CA3. In contrast, double-labeling experiments in rodents revealed that neocortical and hippocampal interneurons expressing GAD67 were consistently devoid of NG. In addition, by using antibodies against PV, CB, CR, we could demonstrate the absence of NG in interneurons of monkey frontal cortex and hippocampus. Together these findings corroborate the idea of different calcium signaling pathways in excitatory and inhibitory cells that may contribute to different modes of synaptic plasticity in these neurons	
Spiegel et al. (2013)	Male Long-Evans rats	Y= 6m, O= 24-26m (n not specified)	CA1, CA3, DG (primarily hilar region)	glutamic acid decarboxylase-67 (GAD67), somatostatin, and neuropeptide Y(NPY), and NeuN	NeuN and SOM are primary; avidin-biotin complex is a secondary	Water maze: 3 x day, 8 days	N/A	the numbers of GAD67- and somatostatin-positive interneurons declined with age across multiple fields of the hippocampus, alterations specifically related to the cognitive outcome of aging were observed exclusively in the hilus of the dentate gyrus	

Stanley and Shetty (2004)	Fischer 344	Adult= 7m, Mid-aged= 15m, Aged= 23m (n= 5/group)	all layers of the dentate gyrus and the CA1 and CA3 subfields, stratum oriens and radiatum	GAD-67, NeuN	GAD-67 antibody, goat anti-rabbit peroxidase, mouse NeuN antibody, avidin-biotin complex method	N/A	N/A	Aging in the hippocampus is associated with wide range-ranging decreases in the number of GAD-67 immunopositive interneurons and most of the age-related changes in GAD-67 immunopositive interneuron numbers transpire by middle age, age-related reductions in hippocampal GAD-67 immunopositive interneuron numbers are due to loss of GAD-67 expression in interneurons rather than interneuron degeneration	
Stanley et al. (2012)	Fisher 344 Brown Norway F1 hybrid rats	Y= 3-5m, O= 26-30m (n=5 or 4 per group, unclear)	CA1	NeuN-, GAD-67-, SOM-, and PV	NeuN, GAD-67, mouse anti-parvalbumin, goat anti somatostatin, secondary biotinylated donkey anti-mouse or anti-goat and horseradish peroxidase conjugated streptavidin	N/A	N/A	Aging significantly reduced high K ⁺ /Ca ²⁺ -evoked GABA, but not glutamate efflux in area CA1. Immunostaining revealed a significant loss of GABAergic interneurons, but not inhibitory boutons in stratum oriens and stratum lacunosum moleculare. Somatostatin-immunoreactive oriens-lacunosum moleculare (O-LM) cells, but not parvalbumin-containing interneurons were selectively lost. Oriens-lacunosum moleculare cells project to distal dendrites of CA1 pyramidal cells, providing dendritic inhibition. Accordingly, inhibition of dendritic input to CA1 from entorhinal cortex was selectively reduced	While it is recognized that the dorsal and ventral hippocampus are functionally dissimilar, our data imply that similar age-related reductions in GABAergic properties may occur in both regions
van de Nes et al. (2002)	Human brains	age 27-93, (n= 24)	hippocampal formation and entorhinal region	SOM	Gallyas silver iodide method, monoclonal antibody AT8 against tau, AT8 in combo with SOM anti serum S209	N/A	N/A	a distinctive interstitial cell type characterized by extensive arborization oriented perpendicular to the course of the perforant pathway and showing somatostatin expression is susceptible to developing the Alzheimer's disease-related cytoskeletal changes. Progression in cytoskeleton change is accompanied by loss of somatostatin	
Vela et al. (2003)	Wistar rats	Y= 3m, A= 24m (n= 4/5 unclear)	CA1, CA2 and CA3, and dentate gyrus	glutamic acid decarboxylase enzymes, parvalbumin, calcitonin, somatostatin, neuropeptide Y and vasoactive intestinal peptide (VIP)	CR goat polyclonal antiserum, monoclonal antibody, SOM rabbit antiserum; secondary, anti-goat IgG, anti-mouse IgG, anti-rabbit IgG	N/A	RNA extraction w/ PCR analysis	There was a differential age-related decrease in the interneuronal mRNAs that was inversely correlated with up-regulation of the $\alpha 1$ GABA receptor subunit. Somatostatin and neuropeptide Y mRNAs were most frequently affected (75% of the animals), then calcitonin and VIP mRNAs (50% of the animals), and parvalbumin mRNA (25% of the animals) in the aged hippocampus.	This age-dependent differential reduction of specific hippocampal interneuronal subpopulations might produce functional alterations in the GABAergic tone which might be compensated, at the post-synaptic level, by up-regulation of the expression of the $\alpha 1$ GABA _A receptor subunit
Aging causes aged rats with cognitive impairment, CA3 pyramidal neurons have elevated firing rates along with a loss in the ability to encode new information (Wilson et al., 2005)									
CA3/dentate gyrus network excitability is also elevated in aged Fisher 344 rats (Patrylo et al., 2007)									